

Fully Conservative Higher Order Finite Difference Schemes for Incompressible Flow

Y. Morinishi,¹ T. S. Lund, O. V. Vasilyev, and P. Moin

Center for Turbulence Research, Stanford University, Stanford, California 94305

Received September 9, 1997; revised February 24, 1998

Conservation properties of the mass, momentum, and kinetic energy equations for incompressible flow are specified as analytical requirements for a proper set of discrete equations. Existing finite difference schemes in regular and staggered grid systems are checked for violations of the conservation requirements and a few important discrepancies are pointed out. In particular, it is found that none of the existing higher order schemes for a staggered mesh system simultaneously conserve mass, momentum, and kinetic energy. This deficiency is corrected through the derivation of a general family of fully conservative higher order accurate finite difference schemes for staggered grid systems. Finite difference schemes in a collocated grid system are also analyzed, and a violation of kinetic energy conservation is revealed. The predicted conservation properties are demonstrated numerically in simulations of inviscid white noise, performed in a two-dimensional periodic domain. The proposed fourth order schemes in a staggered grid system are generalized for the case of a non-uniform mesh, and the resulting scheme is used to perform large eddy simulations of turbulent channel flow. © 1998 Academic Press

1. INTRODUCTION

The purpose of this research is to construct accurate finite difference schemes for incompressible unsteady turbulent flow simulations such as large eddy simulation (LES) or direct numerical simulation (DNS). Experience has shown that the convective terms must conserve kinetic energy if an incompressible, unsteady flow simulation is to be both stable and free of numerical dissipation. Arakawa [1] showed that when central differences are used, conservation of enstrophy in the absence of viscous dissipation is required for long time integration in the two-dimensional vorticity-streamfunction formulation. The corresponding

¹ Permanent affiliation: Department of Mechanical Engineering, Nagoya Institute of Technology, Gokiso-cho, Showa-ku, Nagoya, 466, Japan.

conserved variable is kinetic energy in the velocity-pressure formulation, and some energy conservative finite difference schemes have been developed for the Navier–Stokes equations in three dimensions. Staggered grid systems are usually required to obtain physically correct pressure fields. The standard second order accurate finite difference scheme [2] in a staggered grid system conserves kinetic energy and this scheme has proven useful for LES and DNS. However, the accuracy of the second order finite difference scheme is low and fine meshes are required [3]. Existing fourth order accurate convective schemes [4, 5] for the staggered grid system do not conserve kinetic energy. As we shall show later, these schemes produce erroneous results at sufficiently high Reynolds number. Higher order staggered grid schemes that conserve kinetic energy have not been presented in the literature.

The conservation of kinetic energy is a consequence of the Navier–Stokes equations for incompressible flow in the inviscid limit. In contrast, kinetic energy conservation in a discrete sense is not a consequence of discrete momentum and discrete mass conservation. It is possible to derive numerical schemes that conserve both mass and momentum but not kinetic energy. It is also possible to derive schemes that conserve kinetic energy even though mass or momentum is not conserved. When kinetic energy is not conserved, two possibilities exist; (1) the errors are strictly dissipative and the simulation is stable or (2) the sign of the error is undetermined and the simulation is generally unstable. Upwind schemes fall into the first category. While these schemes are popular, their associated numerical dissipation adds a non-physical damping mechanism to the Navier–Stokes equations. This damping is acceptable in cases where the solution is expected to be smooth (such as in solutions to the laminar or time-averaged Navier–Stokes equations). Unsteady, three-dimensional turbulent simulations are much less tolerant of numerical dissipation [6] since it selectively removes energy from the dynamically important small-scale eddies. For this reason, non-dissipative central-difference schemes or spectral methods [7] are usually preferred for turbulent simulations. Although central difference schemes do not give rise to numerical dissipation in general, they may not conserve kinetic energy. Most often non-conservative central difference schemes are unstable, but this instability may not be apparent unless the Reynolds number is sufficiently high. There are several examples in the literature where non-conservative schemes are presented and tested only for low Reynolds number. We shall show a few examples where these schemes become unstable as the Reynolds number is increased. These schemes can be particularly dangerous at intermediate Reynolds numbers, where the simulation is stable but adversely affected by the conservation errors.

The paper is organized as follows. Conservation properties of the mass, momentum, and kinetic energy equations for incompressible flow are reviewed in Section 2. These conservation properties are regarded as analytical requirements for a proper set of discrete equations. Discrete operators used in this paper are defined in Section 3. Existing finite difference schemes in a regular grid system are checked for violations of the conservation properties in Section 4. In Section 5 we analyze existing staggered grid schemes and propose a new class of conservative schemes. Finite difference schemes for a collocated grid system, which have been used in recent unsteady incompressible flow simulations, are discussed in Section 6. Generalization of the proposed staggered-mesh fourth order accurate scheme to a non-uniform mesh is presented in Section 7. The treatment of non-periodic boundary conditions is also discussed in this section. Finally, numerical tests of the conservation properties and the accuracy of different numerical algorithms are performed in Section 8. Conservation properties of the numerical schemes are demonstrated on the example of two-dimensional, periodic, inviscid white noise simulations. The accuracy of the numerical

algorithm for non-uniform mesh is verified through numerical tests involving the growth of instability eigenfunctions in two-dimensional plane channel flow. Large eddy simulations of turbulent channel flow are performed there as well and the results of the new fourth order accurate schemes are compared with those of the second order accurate algorithm.

2. ANALYTICAL REQUIREMENTS

The continuity and momentum equation describe the motion of incompressible flow. These equations are written symbolically as

$$(Cont.) = 0, \quad (1)$$

$$\frac{\partial v_i}{\partial t} + (Conv.)_i + (Pres.)_i + (Visc.)_i = 0, \quad (2)$$

where

$$(Cont.) \equiv \frac{\partial v_i}{\partial x_i}, \quad (3)$$

$$(Pres.)_i \equiv \frac{\partial p}{\partial x_i}, \quad (4)$$

$$(Visc.)_i \equiv \frac{\partial \tau_{ij}}{\partial x_j}, \quad (5)$$

where v_i is the velocity vector, p is the pressure divided by density and τ_{ij} is the viscous stress. Henceforth, p will be referred to as pressure. $(Conv.)_i$ is a generic form of the convective term and will be defined below.

The conservation properties of Eqs. (1) and (2) will now be established. Note that Eqs. (1) and (2) are of the form

$$\frac{\partial \phi}{\partial t} + {}^1Q(\phi) + {}^2Q(\phi) + {}^3Q(\phi) + \dots = 0. \quad (6)$$

The term ${}^kQ(\phi)$ is *conservative* if it can be written in divergence form,

$${}^kQ(\phi) = \nabla \cdot ({}^kF(\phi)) = \frac{\partial ({}^kF_j(\phi))}{\partial x_j}. \quad (7)$$

To see that the divergence form is conservative, integrate Eq. (6) over the volume and make use of Gauss's theorem for the flux terms $k = 1, 2, \dots$, all of which are assumed to satisfy Eq. (7):

$$\frac{\partial}{\partial t} \iiint_V \phi \, dV = - \iint_S ({}^1F(\phi) + {}^2F(\phi) + {}^3F(\phi) + \dots) \cdot dS. \quad (8)$$

From Eq. (8), we notice that the time derivative of the sum of ϕ in a volume V equals the sum of the flux ${}^kF(\phi)$ on the surface S of the volume. In particular, the sum of ϕ never changes in periodic field if ${}^kQ(\phi)$ is conservative for all k .

Note that mass is conserved *a priori* since the continuity appears in divergence form. By the same token, the pressure $(Pres.)_i$ and viscous terms $(Visc.)_i$ are conservative *a priori* in the momentum equation. The convective term is also conservative *a priori* if it is cast

in divergence form. This is not always the case, however, and we shall investigate it cast in alternative forms. To perform the analysis, we regard $(Conv.)_i$ as a generic form of the convective term in the momentum equation. At least four types of convective forms are often used in analytical or numerical studies. These forms are defined as

$$(Div.)_i \equiv \frac{\partial v_j v_i}{\partial x_j}, \quad (9)$$

$$(Adv.)_i \equiv v_j \frac{\partial v_i}{\partial x_j}, \quad (10)$$

$$(Skew.)_i \equiv \frac{1}{2} \frac{\partial v_j v_i}{\partial x_j} + \frac{1}{2} v_j \frac{\partial v_i}{\partial x_j}, \quad (11)$$

$$(Rot.)_i \equiv v_j \left(\frac{\partial v_i}{\partial x_j} - \frac{\partial v_j}{\partial x_i} \right) + \frac{1}{2} \frac{\partial v_j v_j}{\partial x_i}, \quad (12)$$

where $(Div.)_i$, $(Adv.)_i$, $(Skew.)_i$, and $(Rot.)_i$ are referred to as *divergence*, *advective*, *skew-symmetric*, and *rotational* forms, respectively. As mentioned above, the *divergence* form is conservative *a priori*. The four forms are connected with each other through the following analytical relations:

$$(Adv.)_i = (Div.)_i - v_i \cdot (Cont.), \quad (13)$$

$$(Skew.)_i = \frac{1}{2} (Div.)_i + \frac{1}{2} (Adv.)_i, \quad (14)$$

$$(Rot.)_i = (Adv.)_i. \quad (15)$$

We note that, analytically, there are only two independent convective forms, and the two are equivalent if $(Cont.) = 0$. It is also apparent that the advective, skew-symmetric, and rotational forms are conservative as long as the continuity equation is satisfied. From Eqs. (13) and (14), we can derive the relations

$$\begin{aligned} (Skew.)_i &= (Div.)_i - \frac{1}{2} v_i \cdot (Cont.) \\ &= (Adv.)_i + \frac{1}{2} v_i \cdot (Cont.). \end{aligned} \quad (16)$$

The transport equation of the square of a velocity component, for instance, $v_1^2/2$, is v_1 times the $i = 1$ component of Eq. (2):

$$\frac{\partial v_1^2/2}{\partial t} + v_1 \cdot (Conv.)_1 + v_1 \cdot (Pres.)_1 + v_1 \cdot (Visc.)_1 = 0. \quad (17)$$

In the above equation, the convective term can be rewritten in the following forms corresponding to those in the momentum equation,

$$v_1 \cdot (Div.)_1 = \frac{\partial v_j v_1^2/2}{\partial x_j} + \frac{1}{2} v_1^2 \cdot (Cont.), \quad (18)$$

$$v_1 \cdot (Adv.)_1 = \frac{\partial v_j v_1^2/2}{\partial x_j} - \frac{1}{2} v_1^2 \cdot (Cont.), \quad (19)$$

$$v_1 \cdot (Skew.)_1 = \frac{\partial v_j v_1^2/2}{\partial x_j}. \quad (20)$$

Note that the skew-symmetric form is conservative *a priori* in the velocity square equation. Since the rotational form is equivalent to the advective form, the four convective forms are energy conservative if $(Cont.) = 0$.

The terms involving pressure and viscous stress in Eq. (17) can be rewritten in the forms

$$v_1 \cdot (Pres.)_1 = \frac{\partial p v_1}{\partial x_1} - p \frac{\partial v_1}{\partial x_1}, \quad (21)$$

$$v_1 \cdot (Visc.)_1 = \frac{\partial \tau_{1j} v_1}{\partial x_j} - \tau_{1j} \frac{\partial v_1}{\partial x_j}. \quad (22)$$

These terms are not conservative since they involve components of the pressure-strain and viscous dissipation.

We can determine the conservation properties of $v_2^2/2$ and $v_3^2/2$ in the same manner as for $v_1^2/2$. The transport equation of kinetic energy, $K \equiv v_i v_i/2$, is v_i times the i -component of Eq. (2) with summation over i :

$$\frac{\partial K}{\partial t} + v_i \cdot (Conv.)_i + v_i \cdot (Pres.)_i + v_i \cdot (Visc.)_i = 0. \quad (23)$$

In Eq. (23), the conservation property of the convective term is determined in the same manner as for $v_1^2/2$. In addition, the terms involving pressure and viscous stress in Eq. (23) can be rewritten into the forms

$$v_i \cdot (Pres.)_i = \frac{\partial p v_i}{\partial x_i} - p \cdot (Cont.), \quad (24)$$

$$v_i \cdot (Visc.)_i = \frac{\partial \tau_{ij} v_i}{\partial x_j} - \tau_{ij} \frac{\partial v_i}{\partial x_j}. \quad (25)$$

The pressure term in Eq. (23) is conservative if $(Cont.) = 0$. The viscous stress term in Eq. (25) is not conservative because the second term on the right-hand side of Eq. (25) is the kinetic energy dissipation. Table 1 provides a summary of the conservation properties of the convective, pressure, and viscous terms in the transport equations of v_i , $v_1^2/2$, and K for incompressible flow.

The objective of this work is to derive higher order accurate finite difference schemes that satisfy these properties in a discrete sense.

TABLE 1
Conservation Properties of the Convective, Pressure, and Viscous
Terms in the v_i , $v_1^2/2$, and K Equations

Terms in momentum eq.	Transport equations		
	v_i	$v_1^2/2$	K
(Div.)	○	○	○
(Adv.) = (Rot.)	○	○	○
(Skew.)	○	○	○
(Pres.)	○	×	○
(Visc.)	○	×	×

Note. ○ is conservative *a priori*, ○ is conservative if $(Cont.) = 0$, and × is not conservative.

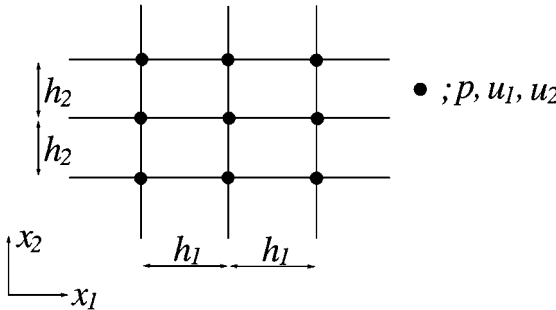


FIG. 1. Regular grid system.

3. DISCRETE OPERATORS

In this and the next three sections, analysis is limited to a uniform grid system, i.e., the grid spacings in each direction, h_1, h_2, h_3 , are constant. A generalization to non-uniform meshes is presented in Section 7.

Conventional numerical algorithms based on a structured computational grid mostly fall into three classes: *regular*, *staggered*, and *collocated* grid systems. In the regular grid system the velocity components u_i ($i = 1, 2, 3$) and pressure p are stored at the same points. The discretization of the continuity and momentum equation are centered at these points. An example of a regular grid system in a two-dimensional plane is shown in Fig. 1. In the staggered grid system the velocity components U_i ($i = 1, 2, 3$) are distributed around the pressure points. The continuity is centered at pressure points. The momentum equation corresponding to each velocity component is centered at the respective velocity point. An example of a staggered grid system in a two-dimensional plane is shown in Fig. 2. In the collocated grid system the velocity components u_i ($i = 1, 2, 3$) and pressure p are defined at the same points, as in the regular grid system. The distinction comes through the definition of an auxiliary *flux velocity*, F_i ($i = 1, 2, 3$), which is obtained via interpolation. The flux velocity is distributed in space as in the staggered grid system. An example of a collocated grid system in a two-dimensional plane is shown in Fig. 3.

Let the finite difference operator with stencil n acting on ϕ with respect to x_1 be defined as

$$\left. \frac{\delta_n \phi}{\delta_n x_1} \right|_{x_1, x_2, x_3} \equiv \frac{\phi(x_1 + nh_1/2, x_2, x_3) - \phi(x_1 - nh_1/2, x_2, x_3)}{nh_1}. \quad (26)$$

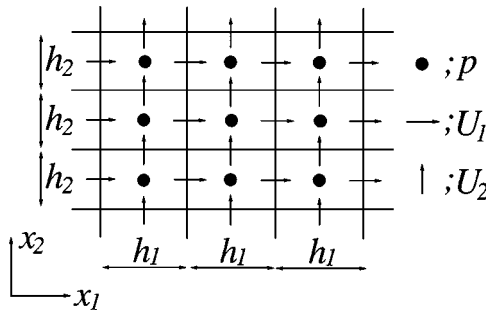


FIG. 2. Staggered grid system.

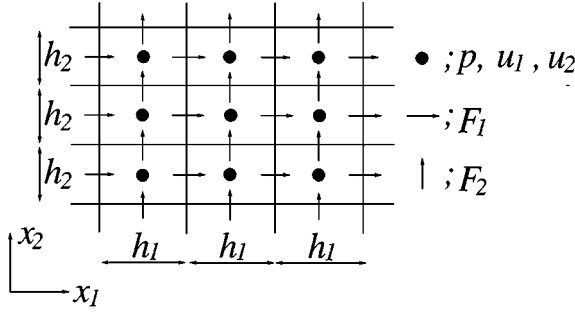


FIG. 3. Collocated grid system.

Also, we define an interpolation operator with stencil n acting on ϕ in the x_1 direction as

$$\bar{\phi}^{nx_1}|_{x_1, x_2, x_3} \equiv \frac{\phi(x_1 + nh_1/2, x_2, x_3) + \phi(x_1 - nh_1/2, x_2, x_3)}{2}. \quad (27)$$

In addition, we define a special interpolation operator with stencil n of the product of ϕ and ψ in the x_1 direction,

$$\begin{aligned} \widetilde{\phi\psi}^{nx_1}|_{x_1, x_2, x_3} &\equiv \frac{1}{2}\phi(x_1 + nh_1/2, x_2, x_3)\psi(x_1 - nh_1/2, x_2, x_3) \\ &+ \frac{1}{2}\psi(x_1 + nh_1/2, x_2, x_3)\phi(x_1 - nh_1/2, x_2, x_3). \end{aligned} \quad (28)$$

Equations (26) and (27) are second order accurate approximations to the first derivative and function value, respectively,

$$\frac{\delta_n \phi}{\delta_n x_1} \simeq \frac{\partial \phi}{\partial x_1} + \frac{n^2}{24} \frac{\partial^3 \phi}{\partial x_1^3} h_1^2 + \frac{n^4}{1920} \frac{\partial^5 \phi}{\partial x_1^5} h_1^4 + \dots, \quad (29)$$

$$\bar{\phi}^{nx_1} \simeq \phi + \frac{n^2}{8} \frac{\partial^2 \phi}{\partial x_1^2} h_1^2 + \frac{n^4}{384} \frac{\partial^4 \phi}{\partial x_1^4} h_1^4 + \dots. \quad (30)$$

Combinations of the discrete operators can be used to make higher order accurate approximations to the first derivative and function value. For example, fourth order accurate approximations to the first derivative can be constructed as

$$\frac{4}{3} \frac{\delta_1 \phi}{\delta_1 x_1} - \frac{1}{3} \frac{\delta_2 \phi}{\delta_2 x_1} \simeq \frac{\partial \phi}{\partial x_1} - \frac{1}{480} \frac{\partial^5 \phi}{\partial x_1^5} h_1^4 + \dots, \quad (31)$$

$$\frac{9}{8} \frac{\delta_1 \phi}{\delta_1 x_1} - \frac{1}{8} \frac{\delta_3 \phi}{\delta_3 x_1} \simeq \frac{\partial \phi}{\partial x_1} - \frac{3}{640} \frac{\partial^5 \phi}{\partial x_1^5} h_1^4 + \dots, \quad (32)$$

$$\frac{4}{3} \frac{\delta_2 \phi}{\delta_2 x_1} - \frac{1}{3} \frac{\delta_4 \phi}{\delta_4 x_1} \simeq \frac{\partial \phi}{\partial x_1} - \frac{1}{30} \frac{\partial^5 \phi}{\partial x_1^5} h_1^4 + \dots. \quad (33)$$

Two fourth order accurate interpolations are

$$\frac{4}{3} \bar{\phi}^{1x_1} - \frac{1}{3} \bar{\phi}^{2x_1} \simeq \phi - \frac{1}{96} \frac{\partial^4 \phi}{\partial x_1^4} h_1^4 + \dots, \quad (34)$$

$$\frac{9}{8} \bar{\phi}^{1x_1} - \frac{1}{8} \bar{\phi}^{3x_1} \simeq \phi - \frac{3}{128} \frac{\partial^4 \phi}{\partial x_1^4} h_1^4 + \dots. \quad (35)$$

Discrete operators in the x_2 and x_3 directions are defined in the same way as for the x_1 direction.

The following identities will be needed to derive some relations later in the paper:

$$\frac{\delta_n \widetilde{\phi} \widetilde{\psi}^{nx_j}}{\delta_n x_j} = \phi \frac{\delta_{2n} \psi}{\delta_{2n} x_j} + \psi \frac{\delta_{2n} \phi}{\delta_{2n} x_j}, \quad (36)$$

$$[(\phi \widetilde{\psi}) \cdot \widetilde{\psi}]^{nx_j} = \widetilde{\phi}^{nx_j} \widetilde{\psi} \widetilde{\psi}^{nx_j}, \quad (37)$$

$$\widetilde{\phi}^{nx_j} \widetilde{\psi}^{nx_j} = \frac{1}{2} \overline{\phi \psi}^{nx_j} + \frac{1}{2} \widetilde{\phi} \widetilde{\psi}^{nx_j}, \quad (38)$$

$$\frac{\delta_n \widetilde{\phi}^{nx_j}}{\delta_n x_j} = \frac{\delta_{2n} \phi}{\delta_{2n} x_j}, \quad (39)$$

$$\frac{\delta_n \widetilde{\phi}^{mx_i}}{\delta_n x_j} = \frac{\overline{\delta_n \phi}^{mx_i}}{\delta_n x_j}, \quad (40)$$

$$\overline{\psi \frac{\delta_n \phi}{\delta_n x_j}}^{nx_j} = \frac{\delta_n \psi \cdot \widetilde{\phi}^{nx_j}}{\delta_n x_j} - \phi \frac{\delta_n \psi}{\delta_n x_j}, \quad (41)$$

$$\phi \frac{\delta_n \psi \cdot \widetilde{\phi}^{nx_j}}{\delta_n x_j} = \frac{1}{2} \frac{\delta_n \psi \cdot \widetilde{\phi} \widetilde{\phi}^{nx_j}}{\delta_n x_j} + \frac{1}{2} \phi \widetilde{\phi} \frac{\delta_n \psi}{\delta_n x_j}. \quad (42)$$

Note that x_j appearing as a superscript does not follow the summation convention.

We define two types of conservative forms in the discrete systems. ${}^k Q(\phi)$ in Eq. (6) is (*locally*) *conservative* if the term can be written as

$${}^k Q(\phi) = \frac{\delta_1({}^k F_j^1(\phi))}{\delta_1 x_j} + \frac{\delta_2({}^k F_j^2(\phi))}{\delta_2 x_j} + \frac{\delta_3({}^k F_j^3(\phi))}{\delta_3 x_j} + \dots \quad (43)$$

This definition corresponds to the analytical conservative form of Eq. (7).

${}^k Q(\phi)$ is *globally conservative* if the following relation holds in a periodic field,

$$\sum_{x_1} \sum_{x_2} \sum_{x_3} {}^k Q(\phi) \Delta V = 0, \quad (44)$$

where the sums that appear in Eq. (44) are taken over the periods in the respective directions and $\Delta V \equiv h_1 h_2 h_3$ is a constant in a uniform grid system. Note that in the periodic case local conservation also implies global conservation. Also note that the definition (44) is a discrete analogue of Eq. (8).

4. FINITE DIFFERENCE SCHEMES IN A REGULAR GRID SYSTEM

4.1. Continuity and Pressure Terms in a Regular Grid System

We first examine the conservation property of the pressure term. As we have observed, the pressure term is analytically conservative in the transport equations of momentum and kinetic energy.

In the regular grid system, the discrete continuity and pressure term are defined as

$$(Cont. - R2) \equiv \frac{\delta_2 u_i}{\delta_2 x_i} = 0, \quad (45)$$

$$(Pres. - R2)_i \equiv \frac{\delta_2 p}{\delta_2 x_i}, \quad (46)$$

where $R2$ denotes a second order accurate approximation in a regular grid system. Fourth order approximations for the continuity and pressure term in the regular grid system are

$$(Cont. - R4) \equiv \frac{4}{3} \frac{\delta_2 u_i}{\delta_2 x_i} - \frac{1}{3} \frac{\delta_4 u_i}{\delta_4 x_i} = 0, \quad (47)$$

$$(Pres. - R4)_i \equiv \frac{4}{3} \frac{\delta_2 p}{\delta_2 x_i} - \frac{1}{3} \frac{\delta_4 p}{\delta_4 x_i}. \quad (48)$$

In the momentum equation, the pressure terms, Eqs. (46) and (48), are conservative *a priori*. Next, consider products of u_i and the pressure terms which appear in Eq. (23). The products can be rewritten using Eq. (36) to give

$$u_i \cdot (Pres. - R2)_i = \frac{\delta_1 \widetilde{u_i p}^{1x_i}}{\delta_1 x_i} - p \cdot (Cont. - R2), \quad (49)$$

$$u_i \cdot (Pres. - R4)_i = \frac{4}{3} \frac{\delta_1 \widetilde{u_i p}^{1x_i}}{\delta_1 x_i} - \frac{1}{3} \frac{\delta_2 \widetilde{u_i p}^{2x_i}}{\delta_2 x_i} - p \cdot (Cont. - R4). \quad (50)$$

These products are conservative provided that the corresponding discrete continuity equations are satisfied. Notice that we need correspondence between the discrete continuity and pressure term to ensure that the pressure term conserves kinetic energy. That is why the residual term in Eq. (49) requires the continuity to be defined as in Eq. (45). It is also important to note that the combination of Eqs. (46) and (47) does not satisfy this property. Table 2 shows a summary of the conservation properties of the discrete pressure terms in a regular grid system.

Before concluding this section, let us consider the Poisson equation for the pressure. The Poisson equation is often solved to satisfy the continuity constraint in computational algorithms of incompressible flow. For example, the projection stage onto a solenoidal field in fractional step methods [8] is

$$v_i^{n+1} = v_i^* - \alpha \Delta t (Pres.)_i, \quad (51)$$

$$(Cont.)^{n+1} = 0. \quad (52)$$

In Eq. (51), Δt is time increment and α is a constant that depends on the time marching method. The superscript refers to the discrete time level and $*$ denotes the non-solenoidal intermediate velocity field. The Poisson equation for the pressure is constructed by substituting

TABLE 2
Conservation Properties of Finite Difference Schemes
for the Pressure Term in a Regular Grid System

	Transport equations	
FD schemes for momentum eq.	u_i	K
$(Pres. - R2)$	\odot	\bigcirc_2
$(Pres. - R4)$	\odot	\bigcirc_4

Note. \odot is conservative *a priori*, \bigcirc_2 is locally conservative if $(Cont. - R2) = 0$, \bigcirc_4 is locally conservative if $(Cont. - R4) = 0$.

Eq. (51) into Eq. (52) in a discrete sense. As we have seen, the proper correspondence between $(Pres.)_i$ and $(Cont.)$ should be used.

The proper combination for the second order scheme in the regular grid system, Eqs. (45) and (46), gives us the following discrete Poisson equation for the pressure:

$$\frac{\delta_2}{\delta_2 x_i} \left(\frac{\delta_2 p}{\delta_2 x_i} \right) = \frac{1}{\alpha \Delta t} (Cont. - R2)^*. \quad (53)$$

The left-hand side of Eq. (53) generates a penta-diagonal matrix for a one-dimensional problem. The solution for pressure using Eq. (53) may not be physical, due to even-odd decoupling. The proper combination for a fourth order scheme in the regular grid system, Eqs. (47) and (48), gives the following discrete Poisson equation for the pressure:

$$\frac{4}{3} \frac{\delta_2}{\delta_2 x_i} \left(\frac{4}{3} \frac{\delta_2 p}{\delta_2 x_i} - \frac{1}{3} \frac{\delta_4 p}{\delta_4 x_i} \right) - \frac{1}{3} \frac{\delta_4}{\delta_4 x_i} \left(\frac{4}{3} \frac{\delta_2 p}{\delta_2 x_i} - \frac{1}{3} \frac{\delta_4 p}{\delta_4 x_i} \right) = \frac{1}{\alpha \Delta t} (Cont. - R4)^*. \quad (54)$$

The left-hand side of Eq. (54) generates a non-diagonal (9 band) matrix for a one-dimensional problem. The matrix has even-odd coupling, but the coupling is weak. Therefore, the pressure given by Eq. (54) may not be physical.

Due to the problem of odd-even decoupling, a staggered grid system is preferred over the regular grid system when a Poisson equation is solved for the pressure. Computational algorithms without the Poisson equation (for example, [9, 10]) can be constructed, however, and it is of interest to consider the conservation properties of such schemes.

4.2. Standard Second Order Accurate Convective Schemes in a Regular Grid System

Here we are interested in conservation properties of convective schemes. The usual second order accurate convective schemes in a regular grid system are defined as

$$(Div. - R2S)_i \equiv \frac{\delta_2 u_j u_i}{\delta_2 x_j}, \quad (55)$$

$$(Adv. - R2S)_i \equiv u_j \frac{\delta_2 u_i}{\delta_2 x_j}, \quad (56)$$

$$(Skew. - R2)_i \equiv \frac{1}{2} \frac{\delta_2 u_j u_i}{\delta_2 x_j} + \frac{1}{2} u_j \frac{\delta_2 u_i}{\delta_2 x_j}, \quad (57)$$

$$(Rot. - R2S)_i \equiv u_j \left(\frac{\delta_2 u_i}{\delta_2 x_j} - \frac{\delta_2 u_j}{\delta_2 x_i} \right) + \frac{1}{2} \frac{\delta_2 u_j u_j}{\delta_2 x_i}. \quad (58)$$

These schemes are direct applications of the standard second order accurate finite difference operator of Eq. (26) to the divergence, advective, skew-symmetric, and rotational forms, respectively ($R2S$ stands for standard second order approximations on a regular grid). $(Div. - R2S)_i$ is conservative *a priori* in the momentum equation. Using Eq. (36), $(Adv. - R2S)_i$ and $(Rot. - R2S)_i$ can be rewritten as

$$(Adv. - R2S)_i = \frac{\widetilde{\delta_1 \bar{u}_j u_i}^{1x_j}}{\delta_1 x_j} - u_i \cdot (Cont. - R2), \quad (59)$$

$$(Rot. - R2S)_i = \frac{\widetilde{\delta_1 \bar{u}_j u_i}^{1x_j}}{\delta_1 x_j} - \frac{1}{2} \frac{\widetilde{\delta_1 \bar{u}_j u_j}^{1x_i}}{\delta_1 x_i} + \frac{1}{2} \frac{\delta_2 u_j u_j}{\delta_2 x_i} - u_i \cdot (Cont. - R2). \quad (60)$$

Therefore, these forms are conservative in the momentum equation if $(Cont. - R2S)_i = 0$.

$(Skew. - R2)_i$ is the average of $(Div. - R2S)_i$ and $(Adv. - R2S)_i$

$$(Skew. - R2)_i = \frac{1}{2}(Div. - R2S)_i + \frac{1}{2}(Adv. - R2S)_i. \quad (61)$$

As a consequence, $(Skew. - R2)_i$ is also conservative in the momentum equation if $(Cont. - R2) = 0$.

Let us investigate the conservation properties of the convective schemes in the transport equation of $u_1^2/2$. It is sufficient to consider the product of u_1 and the $i = 1$ component of the convective schemes. Using Eqs. (36) and (37), this product can be rewritten as

$$u_1 \cdot (Skew. - R2)_1 = \frac{\delta_1 \bar{u}_j^{1x_j} \widetilde{u_1 u_1}^{1x_j} / 2}{\delta_1 x_j}. \quad (62)$$

Therefore, $(Skew. - R2)_1$ is conservative in the $u_1^2/2$ equation. On the other hand, using Eq. (36), the product of u_1 and $(Div. - R2S)_1$ can be rewritten as

$$u_1 \cdot (Div. - R2S)_1 = \frac{\delta_1 (\widetilde{u_1 \cdot u_j} u_1)^{1x_j}}{\delta_1 x_j} - u_j u_1 \frac{\delta_2 u_1}{\delta_2 x_j}.$$

This term is not conservative since the second term on the right-hand side cannot be put in divergence form. It can be shown that $(Adv. - R2S)_1$ and $(Rot. - R2S)_1$ are also not conservative in the $u_1^2/2$ equation. In the same way, we can determine the conservation properties of the convective schemes in the transport equation of kinetic energy, $(K \equiv u_i u_i/2)$. The following relations can be derived:

$$u_i \cdot (Skew. - R2)_i = \frac{\delta_1 \bar{u}_j^{1x_j} \widetilde{u_i u_i}^{1x_j} / 2}{\delta_1 x_j}, \quad (63)$$

$$u_i \cdot (Rot. - R2S)_i = \frac{\delta_1 (\widetilde{u_i \cdot u_j} u_j)^{1x_i} / 2}{\delta_1 x_i} - \frac{1}{2} u_j u_j \cdot (Cont. - R2). \quad (64)$$

$(Skew. - R2)_i$ is conservative *a priori* in the K equation. $(Rot. - R2S)_i$ is conservative in the K equation if $(Cont. - R2) = 0$. $(Div. - R2S)_i$ and $(Adv. - R2S)_i$ are not conservative in the K equation.

Table 3 summarizes the conservation properties of the standard schemes, Eqs. (55), (56), (57), and (58). Comparing Table 3 and Table 1, we see that the only properly discretized

TABLE 3
Conservation Properties of Standard Second Order Accurate
Convective Schemes in a Regular Grid System

FD schemes for momentum eq.	Transport equations		
	u_i	$u_1^2/2$	K
$(Div. - R2S)$	⊕	×	×
$(Adv. - R2S)$	○	×	×
$(Rot. - R2S)$	○	×	○
$(Skew. - R2)$	○	⊕	⊕

Note. ⊕ is conservative *a priori*, ○ is conservative if $(Cont. - R2) = 0$, and × is not conservative.

standard scheme is $(Skew. - R2)_i$. Although $(Rot. - R2S)_i$ is conservative in the momentum and kinetic energy equations, it is not conservative in the equations for the square of the individual velocity components (u_1^2, u_2^2, u_3^2) . This scheme has been used in the past but, as shown by Horiuti [10], leads to excessively large truncation error.

4.3. Fully Conservative Second Order Accurate Convective Schemes in a Regular Grid System

As shown in the previous section, $(Skew. - R2)_i$ is the only fully conservative standard convective scheme for a regular grid system. Fully conservative variants for the divergence and advective forms do exist, but they are different from the forms already considered. These forms can be constructed from $(Skew. - R2)_i$ by adding or subtracting factors of the velocity multiplied by the discrete continuity equation (see Eq. (16)):

$$\begin{aligned} (Skew. - R2)_i &= (Div. - R2)_i - \frac{1}{2} u_i \cdot (Cont. - R2) \\ &= (Adv. - R2)_i + \frac{1}{2} u_i \cdot (Cont. - R2). \end{aligned} \quad (65)$$

By substituting Eqs. (45) and (57) into Eq. (65) and then using Eqs. (36), (38), (39), and (40), the divergence and advective forms that satisfy Eq. (65) are

$$(Div. - R2)_i \equiv \frac{\delta_1 \bar{u}_j^{1x_j} \bar{u}_i^{1x_j}}{\delta_1 x_j}, \quad (66)$$

$$(Adv. - R2)_i \equiv \bar{u}_j^{1x_j} \frac{\delta_1 u_i^{1x_j}}{\delta_1 x_j}. \quad (67)$$

$(Div. - R2)_i$ is a natural divergence form for a control volume centered at the mesh point. $(Div. - R2)_i$ and $(Adv. - R2)_i$ are related to $(Skew. - R2)_i$ through Eq. (65), and they are equivalent if $(Cont. - R2) = 0$. Using this fact, the conservation properties of $(Div. - R2)_i$ and $(Adv. - R2)_i$ are determined by the properties of $(Skew. - R2)_i$. The results are shown in Table 4. The conservation properties of the convective schemes in Table 4 agree with those of Table 1. Therefore, $(Div. - R2)_i$, $(Adv. - R2)_i$, and $(Skew. - R2)_i$ are a *proper set* of convective schemes provided $(Cont. - R2) = 0$. The skew-symmetric form $(Skew. - R2)_i$ is related to the proper divergence and advective forms via

$$(Skew. - R2)_i = \frac{1}{2} (Div. - R2)_i + \frac{1}{2} (Adv. - R2)_i. \quad (68)$$

TABLE 4
Conservation Properties of Proper Second Order Accurate Convective Schemes in a Regular Grid System

FD schemes for momentum eq.	Transport equations		
	u_i	$u_1^2/2$	K
$(Div. - R2)$	○	○	○
$(Adv. - R2)$	○	○	○
$(Skew. - R2)$	○	○	○

Note. Symbols are the same as Table 3.

This relation should be used in place of Eq. (61) since the latter equation relies on a cancellation of errors on the right-hand side in order to arrive at a proper skew-symmetric form. $(Adv. - R2)_i$ is related to $(Div. - R2)_i$ through the following analogue of Eq. (13):

$$(Adv. - R2)_i = (Div. - R2)_i - u_i \cdot (Cont. - R2). \quad (69)$$

According to Eq. (15), the rotational and advective forms are equivalent, thus the following discrete relation is assumed:

$$(Rot. - R2)_i = (Adv. - R2)_i. \quad (70)$$

Starting with Eq. (67) and then using Eqs. (36), (38), (39), and (40), the discrete rotational form that satisfies Eq. (70) is

$$(Rot. - R2)_i = \left(\bar{u}_j^{1x_j} \frac{\delta_1 u_i}{\delta_1 x_j}^{1x_j} - \bar{u}_j^{1x_i} \frac{\delta_1 u_j}{\delta_1 x_i}^{1x_i} \right) + \frac{1}{2} \frac{\delta_2 u_j u_j}{\delta_2 x_i}. \quad (71)$$

Although the above relation is written in a rotational like form, it is equivalent to Eq. (67). Since the two forms are equivalent we shall not discuss the rotational form further.

4.4. Fully Conservative Fourth Order Accurate Convective Schemes for a Regular Grid System

In a regular grid system, proper fourth order accurate convective schemes are obtained via a straightforward extension of the proper second order schemes:

$$(Div. - R4)_i \equiv \frac{4}{3} \frac{\delta_1 \bar{u}_j^{1x_j} \bar{u}_i^{1x_j}}{\delta_1 x_j} - \frac{1}{3} \frac{\delta_2 \bar{u}_j^{2x_j} \bar{u}_i^{2x_j}}{\delta_2 x_j}, \quad (72)$$

$$(Adv. - R4)_i \equiv \frac{4}{3} \bar{u}_j^{1x_j} \frac{\delta_1 u_i}{\delta_1 x_j}^{1x_j} - \frac{1}{3} \bar{u}_j^{2x_j} \frac{\delta_2 u_i}{\delta_2 x_j}^{2x_j}, \quad (73)$$

$$(Skew. - R4)_i \equiv \frac{1}{2} (Div. - R4)_i + \frac{1}{2} (Adv. - R4)_i. \quad (74)$$

$(Div. - R4)_i$ was used by Horiuti [11], and is conservative *a priori* in the momentum equation. Using Eqs. (36) and (37), u_1 times $(Skew. - R4)_i$ can be written as

$$u_1 \cdot (Skew. - R4)_1 = \frac{4}{3} \frac{\delta_1 \bar{u}_j^{1x_j} \widetilde{u_1 u_1}^{1x_j} / 2}{\delta_1 x_j} - \frac{1}{3} \frac{\delta_2 \bar{u}_j^{2x_j} \widetilde{u_1 u_1}^{2x_j} / 2}{\delta_2 x_j}. \quad (75)$$

Therefore, $(Skew. - R4)_i$ is conservative *a priori* in the transport equation of $u_1^2/2$. The conservation property of $(Skew. - R4)_i$ in the transport equation of kinetic energy follows directly. $(Adv. - R4)_i$ and $(Div. - R4)_i$ are connected through the equation

$$(Adv. - R4)_i = (Div. - R4)_i - u_i \cdot (Cont. - R4). \quad (76)$$

As a consequence, $(Div. - R4)_i$, $(Adv. - R4)_i$, and $(Skew. - R4)_i$ are all equivalent if $(Cont. - R4) = 0$, and the conservation properties of $(Adv. - R4)$ and $(Div. - R4)$ can be determined by using Eq. (76). Table 5 summarizes the results. It is evident that these schemes are a proper set of convective schemes provided $(Cont. - R4) = 0$.

TABLE 5
Conservation Properties of Proper Fourth Order Accurate Convective Schemes in a Regular Grid System

FD schemes for momentum eq.	Transport equations		
	u_i	$u_i^2/2$	K
(Div. – R4)	○	○	○
(Adv. – R4)	○	○	○
(Skew. – R4)	○	○	○

Note. ○ is conservative *a priori* and ○ is conservative if (Cont. – R4) = 0.

5. FINITE DIFFERENCE SCHEMES IN A STAGGERED GRID SYSTEM

5.1. Continuity and Pressure Terms in a Staggered Grid System

In a staggered grid system, we define the discrete continuity and pressure terms as

$$(Cont. - S2) \equiv \frac{\delta_1 U_i}{\delta_1 x_i} = 0, \quad (77)$$

$$(Pres. - S2)_i \equiv \frac{\delta_1 p}{\delta_1 x_i}, \quad (78)$$

where the S2 denotes second order accuracy in a staggered grid system. Note that the finite difference stencils cover only one mesh spacing since the derivatives are needed between the nodal values. Analogous fourth order approximations are

$$(Cont. - S4) \equiv \frac{9}{8} \frac{\delta_1 U_i}{\delta_1 x_i} - \frac{1}{8} \frac{\delta_3 U_i}{\delta_3 x_i} = 0, \quad (79)$$

$$(Pres. - S4)_i \equiv \frac{9}{8} \frac{\delta_1 p}{\delta_1 x_i} - \frac{1}{8} \frac{\delta_3 p}{\delta_3 x_i}. \quad (80)$$

Local kinetic energy cannot be defined unambiguously in a staggered grid system since the individual velocity components are defined at different locations in space. Some sort of interpolation must be used in order to obtain the kinetic energy at the same point. The required interpolations for the pressure terms in the K equations are

$$\overline{U_i \frac{\delta_1 p}{\delta_1 x_i}}^{1x_i} = \frac{\delta_1 U_i \bar{p}^{1x_i}}{\delta_1 x_i} - p \cdot (Cont. - S2), \quad (81)$$

$$\frac{9}{8} \overline{U_i \frac{\delta_1 p}{\delta_1 x_i}}^{1x_i} - \frac{1}{8} \overline{U_i \frac{\delta_3 p}{\delta_3 x_i}}^{3x_i} = \frac{9}{8} \frac{\delta_1 U_i \bar{p}^{1x_i}}{\delta_1 x_i} - \frac{1}{8} \frac{\delta_3 U_i \bar{p}^{3x_i}}{\delta_3 x_i} - p \cdot (Cont. - S4). \quad (82)$$

The following relations can be used to show global conservation unambiguously:

$$\sum_{x_1} \sum_{x_2} \sum_{x_3} U_i \cdot (Pres. - S2)_i = \sum_{x_1} \sum_{x_2} \sum_{x_3} \overline{U_i \frac{\delta_1 p}{\delta_1 x_i}}^{1x_i}, \quad (83)$$

$$\sum_{x_1} \sum_{x_2} \sum_{x_3} U_i \cdot (Pres. - S4)_i = \sum_{x_1} \sum_{x_2} \sum_{x_3} \left(\frac{9}{8} \overline{U_i \frac{\delta_1 p}{\delta_1 x_i}}^{1x_i} - \frac{1}{8} \overline{U_i \frac{\delta_3 p}{\delta_3 x_i}}^{3x_i} \right). \quad (84)$$

Therefore, Eqs. (78) and (80) are globally conservative if the corresponding discrete

TABLE 6
Conservation Properties of Finite Difference Schemes
for the Pressure Term in a Staggered Grid System

	Transport equations	
	U_i	K
FD schemes for momentum eq.		
(<i>Pres.</i> – <i>S2</i>)	⊖	⊖ ₂
(<i>Pres.</i> – <i>S4</i>)	⊖	⊖ ₄

Note. ⊖ is conservative *a priori*, ⊖₂ is locally conservative if (*Cont.* – *S2*) = 0, ⊖₄ is locally conservative if (*Cont.* – *S4*) = 0.

continuity equations are satisfied. Table 6 shows a summary of the conservation properties of the discrete pressure term in a staggered grid system.

The proper combination between second order continuity and pressure terms in a staggered grid system, Eqs. (77) and (78), give us the following discretized Poisson equation for the pressure (* refers to the intermediate velocity field in the fractional step scheme; see Eq. (51)):

$$\frac{\delta_1}{\delta_1 x_i} \left(\frac{\delta_1 p}{\delta_1 x_i} \right) = \frac{1}{\alpha \Delta t} (\text{Cont.} - \text{S2})^*. \quad (85)$$

Similarly, the proper combination between fourth order continuity and pressure terms, Eqs. (79) and (80), gives

$$\frac{9}{8} \frac{\delta_1}{\delta_1 x_i} \left(\frac{9}{8} \frac{\delta_1 p}{\delta_1 x_i} - \frac{1}{8} \frac{\delta_3 p}{\delta_3 x_i} \right) - \frac{1}{8} \frac{\delta_3}{\delta_3 x_i} \left(\frac{9}{8} \frac{\delta_1 p}{\delta_1 x_i} - \frac{1}{8} \frac{\delta_3 p}{\delta_3 x_i} \right) = \frac{1}{\alpha \Delta t} (\text{Cont.} - \text{S4})^*. \quad (86)$$

The left-hand side of Eq. (85) results in a tri-diagonal matrix for one-dimensional problems, whereas the left-hand side of Eq. (86) results in a septa-diagonal matrix. Non-oscillatory solutions for the pressure are expected from Eqs. (85) and (86), since both matrices have strong even-odd coupling.

5.2. Proper Second Order Accurate Convective Schemes in a Staggered Grid System

As we have already mentioned, local kinetic energy $K \equiv U_i U_i / 2$ cannot be defined uniquely in a staggered grid system. Let us assume that a term is (locally) conservative in the transport equation of K if the term is (locally) conservative in the transport equations of $U_1^2/2$, $U_2^2/2$, and $U_3^2/2$. Since the conservation properties of $U_2^2/2$ and $U_3^2/2$ are estimated in the same manner as for $U_1^2/2$, only the conservation properties of the convective schemes in the momentum and $U_1^2/2$ equations need to be considered.

Let us define second order accurate convective schemes in a staggered grid system as

$$(\text{Div.} - \text{S2})_i \equiv \frac{\delta_1 \bar{U}_j^{1x_i} \bar{U}_i^{1x_j}}{\delta_1 x_j}, \quad (87)$$

$$(\text{Adv.} - \text{S2})_i \equiv \frac{\bar{U}_j^{1x_i} \delta_1 \bar{U}_i^{1x_j}}{\delta_1 x_j}, \quad (88)$$

$$(\text{Skew.} - \text{S2})_i \equiv \frac{1}{2} (\text{Div.} - \text{S2})_i + \frac{1}{2} (\text{Adv.} - \text{S2})_i. \quad (89)$$

TABLE 7
Conservation Properties of Proper Second Order Accurate Convective Schemes in a Staggered Grid System

FD schemes for momentum eq.	Transport equations		
	U_i	$U_1^2/2$	K
(Div. – S2)	⊕	○	○
(Adv. – S2)	○	○	○
(Skew. – S2)	○	⊕	⊕

Note. ⊕ is conservative *a priori* and ○ is conservative if (Cont. – S2) = 0.

Using Eqs. (40) and (41), $(Adv. – S2)_i$ is connected with $(Div. – S2)_i$ via

$$(Adv. – S2)_i = (Div. – S2)_i - U_i \cdot \overline{(Cont. – S2)}^{1x_i}. \quad (90)$$

$(Div. – S2)_i$ is the standard divergence form in a staggered grid system [2]. $(Adv. – S2)_i$ was proposed by Kajishima [5]. $(Skew. – S2)_i$ is equivalent to the scheme that was proposed by Piacsek and Williams [12].

Clearly $(Div. – S2)_i$ is conservative *a priori* in the momentum equation. Using Eqs. (41) and (42), the product between U_1 and $(Skew. – S2)_1$ can be rewritten as

$$U_1 \cdot (Skew. – S2)_1 = \frac{\delta_1 \bar{U}_j^{1x_1} \widetilde{U_1 U_1}^{1x_j} / 2}{\delta_1 x_j}. \quad (91)$$

Therefore, $(Skew. – S2)_1$ is conservative *a priori* in the transport equation of $U_1^2/2$.

By using Eq. (90), the conservation properties of the various schemes are determined. The results are summarized in Table 7. These schemes are seen to be conservative provided that the continuity equation is satisfied.

5.3. Existing Fourth Order Accurate Convective Schemes in a Staggered Grid System

Before proposing fully conservative fourth order accurate convective schemes, we first examine some existing fourth order schemes in a staggered grid system. By simple extension of the proper second order accurate convective schemes, we obtain the schemes

$$(Div. – S4A)_i \equiv \frac{9}{8} \frac{\delta_1 \bar{U}_j^{1x_i} \bar{U}_i^{1x_j}}{\delta_1 x_j} - \frac{1}{8} \frac{\delta_3 \bar{U}_j^{3x_i} \bar{U}_i^{3x_j}}{\delta_3 x_j}, \quad (92)$$

$$(Adv. – S4A)_i \equiv \frac{9}{8} \frac{\overline{\bar{U}_j^{1x_i} \delta_1 \bar{U}_i^{1x_j}}}{\delta_1 x_j} - \frac{1}{8} \frac{\overline{\bar{U}_j^{3x_i} \delta_3 \bar{U}_i^{3x_j}}}{\delta_3 x_j}, \quad (93)$$

$$(Skew. – S4A)_i \equiv \frac{1}{2} (Div. – S4A)_i + \frac{1}{2} (Adv. – S4A)_i. \quad (94)$$

$(Div. – S4A)_i$ was used by A-Domis [4], and is conservative *a priori* in the momentum equation. Using Eqs. (41) and (42), the product between U_1 and $(Skew. – S4A)_1$ can be

written as

$$U_i \cdot (Skew. - S4A)_1 = \frac{9}{8} \frac{\delta_1 \bar{U}_j^{1x_i} \widetilde{U_1 U_1}^{1x_j} / 2}{\delta_1 x_j} - \frac{1}{8} \frac{\delta_3 \bar{U}_j^{3x_i} \widetilde{U_1 U_1}^{3x_j} / 2}{\delta_3 x_j}. \quad (95)$$

Therefore, $(Skew. - S4A)_1$ is conservative *a priori* in the transport equation of $U_1^2/2$. The difference between $(Adv. - S4A)_i$ and $(Div. - S4A)_i$ is

$$(Adv. - S4A)_i = (Div. - S4A)_i - U_i \cdot \left(\frac{9}{8} \frac{\overline{\delta_1 U_j}^{1x_i}}{\delta_1 x_j} - \frac{1}{8} \frac{\overline{\delta_3 U_j}^{3x_i}}{\delta_3 x_j} \right). \quad (96)$$

This equation is the discrete analogue of Eq. (13). However, $(Adv. - S4A)_i$ is not equal to $(Div. - S4A)_i$, because the term that appears on the right-hand side of Eq. (96) differs from the properly discretized fourth order continuity equation in a staggered grid system (Eq. (79)). The difference between the right-hand side of Eq. (96) and Eq. (79) scales like

$$\left(\frac{9}{8} \frac{\overline{\delta_1 U_j}^{1x_i}}{\delta_1 x_j} - \frac{1}{8} \frac{\overline{\delta_3 U_j}^{3x_i}}{\delta_3 x_j} \right) - (Cont. - S4) = O(h^4), \quad (97)$$

where h is grid spacing. While the error is small it is not zero and therefore $(Adv. - S4A)_i$ does not conserve momentum. As a consequence $(Skew. - S4A)_i$ does not conserve momentum either. Furthermore, using Eqs. (95), (96), and (94) it can be shown that $(Div. - S4A)_i$ and $(Adv. - S4A)_i$ do not conserve $U_1^2/2$. Table 8 shows the conservation properties of $(Div. - S4A)_i$, $(Adv. - S4A)_i$, and $(Skew. - S4A)_i$. It is evident that each of these schemes has one or more conservation defects. In spite of this, it might be expected that some of these schemes could still be used since the errors in the table are $O(h^4)$. Indeed, $(Div. - S4A)_i$ was used in [4] to obtain good results for LES of isotropic decaying turbulence at low Reynolds number. However, we observed numerical instabilities in LES of channel flow at high Reynolds number with the same scheme. The instability may be avoided by using $(Skew. - S4A)_i$ (since it conserves kinetic energy) but momentum would not be conserved in this case.

Another possible set of fourth order accurate convective schemes in a staggered grid system is

$$(Div. - S4K)_i \equiv \frac{9}{8} \frac{\delta_1}{\delta_1 x_j} \left[\left(\frac{9}{8} \bar{U}_j^{1x_i} - \frac{1}{8} \bar{U}_j^{3x_i} \right) \left(\frac{9}{8} \bar{U}_i^{1x_j} - \frac{1}{8} \bar{U}_i^{3x_j} \right) \right] - \frac{1}{8} \frac{\delta_3}{\delta_3 x_j} \left[\left(\frac{9}{8} \bar{U}_j^{1x_i} - \frac{1}{8} \bar{U}_j^{3x_i} \right) \left(\frac{9}{8} \bar{U}_i^{1x_j} - \frac{1}{8} \bar{U}_i^{3x_j} \right) \right], \quad (98)$$

TABLE 8
Conservation Properties of A-Domis Type Fourth Order Accurate
Convective Schemes in a Staggered Grid System

FD schemes for momentum eq.	Transport equations		
	U_i	$U_1^2/2$	K
$(Div. - S4A)$	○	△	△
$(Adv. - S4A)$	△	△	△
$(Skew. - S4A)$	△	○	○

Note. ○ is conservative *a priori*. △ has an error of $O(h^4)$ even if $(Cont. - S4) = 0$.

$$(Adv. - S4K)_i \equiv \frac{9}{8} \overline{\left(\frac{9}{8} \bar{U}_j^{1x_i} - \frac{1}{8} \bar{U}_j^{3x_i} \right)} \left(\frac{9}{8} \frac{\delta_1 U_i}{\delta_1 x_j} - \frac{1}{8} \frac{\delta_3 U_i}{\delta_3 x_j} \right)^{1x_j} - \frac{1}{8} \overline{\left(\frac{9}{8} \bar{U}_j^{1x_i} - \frac{1}{8} \bar{U}_j^{3x_i} \right)} \left(\frac{9}{8} \frac{\delta_1 U_i}{\delta_1 x_j} - \frac{1}{8} \frac{\delta_3 U_i}{\delta_3 x_j} \right)^{3x_j}, \quad (99)$$

$$(Skew. - S4K)_i \equiv \frac{1}{2} (Div. - S4K)_i + \frac{1}{2} (Adv. - S4K)_i. \quad (100)$$

$(Adv. - S4K)_i$ was proposed by Kajishima [5] as the extension of his second order scheme (Eq. (88)). Unfortunately, the conservation properties of Eqs. (98), (99), and (100) are similar to those of Eqs. (92), (93), and (94), and thus each of them has at least one conservation error.

5.4. A Proposal for Fully Conservative, Higher Order Accurate Convective Schemes in a Staggered Grid System

In this section we show how to construct fully conservative convective schemes for a staggered grid system having arbitrary order of accuracy. We start with the following set of fourth order accurate schemes:

$$(Div. - S4)_i \equiv \frac{9}{8} \frac{\delta_1}{\delta_1 x_j} \left[\left(\frac{9}{8} \bar{U}_j^{1x_i} - \frac{1}{8} \bar{U}_j^{3x_i} \right) \bar{U}_i^{1x_i} \right] - \frac{1}{8} \frac{\delta_3}{\delta_3 x_j} \left[\left(\frac{9}{8} \bar{U}_j^{1x_i} - \frac{1}{8} \bar{U}_j^{3x_i} \right) \bar{U}_j^{3x_j} \right], \quad (101)$$

$$(Adv. - S4)_i \equiv \frac{9}{8} \overline{\left(\frac{9}{8} \bar{U}_j^{1x_i} - \frac{1}{8} \bar{U}_j^{3x_i} \right)} \frac{\delta_1 U_i}{\delta_1 x_j}^{1x_j} - \frac{1}{8} \overline{\left(\frac{9}{8} \bar{U}_j^{1x_i} - \frac{1}{8} \bar{U}_j^{3x_i} \right)} \frac{\delta_3 U_i}{\delta_3 x_j}^{3x_j}, \quad (102)$$

$$(Skew. - S4)_i \equiv \frac{1}{2} (Div. - S4)_i + \frac{1}{2} (Adv. - S4)_i. \quad (103)$$

We see that $(Div. - S4)_i$ is conservative *a priori* in the momentum equation. Using Eqs. (41) and (42), the product between U_1 and $(Skew. - S4)_1$ can be rewritten as

$$U_1 \cdot (Skew. - S4)_1 = \frac{9}{8} \frac{\delta_1}{\delta_1 x_j} \left[\left(\frac{9}{8} \bar{U}_j^{1x_1} - \frac{1}{8} \bar{U}_j^{3x_1} \right) \frac{\widetilde{U}_1 U_1}{2}^{1x_j} \right] - \frac{1}{8} \frac{\delta_3}{\delta_3 x_j} \left[\left(\frac{9}{8} \bar{U}_j^{1x_1} - \frac{1}{8} \bar{U}_j^{3x_1} \right) \frac{\widetilde{U}_1 U_1}{2}^{3x_j} \right]. \quad (104)$$

Thus, $(Skew. - S4)_i$ is conservative *a priori* in the transport equation of $U_1^2/2$. Using Eqs. (40) and (41), the relation between $(Adv. - S4)_i$ and $(Div. - S4)_i$ is

$$(Adv. - S4)_i = (Div. - S4)_i - U_i \cdot \left[\frac{9}{8} \overline{(Cont. - S4)}^{1x_i} - \frac{1}{8} \overline{(Cont. - S4)}^{3x_i} \right]. \quad (105)$$

This equation is a proper discrete analog of Eq. (13), and $(Adv. - S4)_i$, $(Div. - S4)_i$ and $(Skew. - S4)_i$ are equivalent if $(Cont. - S4) = 0$. Table 9 shows the conservation properties of the proposed schemes. Comparing Table 9 with Table 1, we see that the present schemes are fully conservative provided that the discrete continuity relation is satisfied.

TABLE 9
Conservation Properties of Proper Fourth Order Accurate Convective Schemes in a Staggered Grid System

FD schemes for momentum eq.	Transport equations		
	U_i	$U_i^2/2$	K
(Div. – S4)	⊕	○	○
(Adv. – S4)	○	○	○
(Skew. – S4)	○	⊕	⊕

Note. ⊕ is conservative *a priori* and ○ is conservative if (Cont. – S4) = 0.

Higher order fully conservative finite difference schemes can be constructed in the same way as for the fourth order schemes. The pattern for a n th order accurate scheme can be seen most clearly in the divergence form. The basic procedure is to make multiple evaluations of the convective term on stencils spanning $1, 3, \dots, n - 1$ mesh spacings and then combine the results with the appropriate n th order accurate interpolation operator. In making the evaluation on stencil of size m , the convection velocity must be interpolated with the n th order accurate interpolation operator, whereas the flux velocity must be interpolated with a 2nd order operator having a m -point stencil. Thus in general we can write

$$(Div. - Sn)_i \equiv \sum_{k=1}^{n/2} \alpha_k \frac{\delta_{(2k-1)}}{\delta_{(2k-1)} x_j} \left[\left(\sum_{l=1}^{n/2} \alpha_l \bar{U}_j^{(2l-1)x_i} \right) (\bar{U}_j^{(2k-1)x_j}) \right], \quad (106)$$

where the α_k are the interpolation weights (see Eqs. (32) and (35)). A similar general formula exists for the advective form

$$(Adv. - Sn)_i \equiv \sum_{k=1}^{n/2} \alpha_k \left(\sum_{l=1}^{n/2} \alpha_l \bar{U}_j^{(2l-1)x_i} \right) \frac{\delta_{(2k-1)} U_i}{\delta_{(2k-1)} x_j}^{(2k-1)x_j}. \quad (107)$$

The continuity and pressure terms involve straightforward applications of the higher order interpolation operators:

$$(Cont. - Sn) \equiv \sum_{k=1}^{n/2} \alpha_k \frac{\delta_{(2k-1)} U_i}{\delta_{(2k-1)} x_i} = 0, \quad (108)$$

$$(Pres. - Sn)_i \equiv \sum_{k=1}^{n/2} \alpha_k \frac{\delta_{(2k-1)} p}{\delta_{(2k-1)} x_i}. \quad (109)$$

As an example, the proper set of sixth order schemes in a staggered grid system is

$$(Cont. - S6) \equiv \frac{150}{128} \frac{\delta_1 U_i}{\delta_1 x_i} - \frac{25}{128} \frac{\delta_3 U_i}{\delta_3 x_i} + \frac{3}{128} \frac{\delta_5 U_i}{\delta_5 x_i} = 0, \quad (110)$$

$$(Pres. - S6)_i \equiv \frac{150}{128} \frac{\delta_1 p}{\delta_1 x_i} - \frac{25}{128} \frac{\delta_3 p}{\delta_3 x_i} + \frac{3}{128} \frac{\delta_5 p}{\delta_5 x_i}, \quad (111)$$

$$(Div. - S6)_i \equiv \frac{150}{128} \frac{\delta_1}{\delta_1 x_j} \left[\left(\frac{150}{128} \bar{U}_j^{1x_i} - \frac{25}{128} \bar{U}_j^{3x_i} + \frac{3}{128} \bar{U}_j^{5x_i} \right) \bar{U}_i^{1x_j} \right] \\ - \frac{25}{128} \frac{\delta_3}{\delta_3 x_j} \left[\left(\frac{150}{128} \bar{U}_j^{1x_i} - \frac{25}{128} \bar{U}_j^{3x_i} + \frac{3}{128} \bar{U}_j^{5x_i} \right) \bar{U}_i^{3x_j} \right] \\ + \frac{3}{128} \frac{\delta_5}{\delta_5 x_j} \left[\left(\frac{150}{128} \bar{U}_j^{1x_i} - \frac{25}{128} \bar{U}_j^{3x_i} + \frac{3}{128} \bar{U}_j^{5x_i} \right) \bar{U}_i^{5x_j} \right], \quad (112)$$

$$(Adv. - S6)_i \equiv \frac{150}{128} \overline{\left(\frac{150}{128} \bar{U}_j^{1x_i} - \frac{25}{128} \bar{U}_j^{3x_i} + \frac{3}{128} \bar{U}_j^{5x_i} \right)} \frac{\delta_1 \bar{U}_i^{1x_j}}{\delta_1 x_j} \\ - \frac{25}{128} \overline{\left(\frac{150}{128} \bar{U}_j^{1x_i} - \frac{25}{128} \bar{U}_j^{3x_i} + \frac{3}{128} \bar{U}_j^{5x_i} \right)} \frac{\delta_3 \bar{U}_i^{3x_j}}{\delta_3 x_j} \\ + \frac{3}{128} \overline{\left(\frac{150}{128} \bar{U}_j^{1x_i} - \frac{25}{128} \bar{U}_j^{3x_i} + \frac{3}{128} \bar{U}_j^{5x_i} \right)} \frac{\delta_5 \bar{U}_i^{5x_j}}{\delta_5 x_j}, \quad (113)$$

$$(Skew. - S6)_i \equiv \frac{1}{2} (Div. - S6)_i + \frac{1}{2} (Adv. - S6)_i. \quad (114)$$

6. FINITE DIFFERENCE SCHEMES IN A COLLOCATED GRID SYSTEM

The main advantage of a staggered grid system is that it results in a non-oscillatory pressure field. On the other hand, a regular grid system is convenient in a curvilinear grid system. A *collocated* grid system supposedly has the merits of both regular and staggered grid systems, and has mainly been used for steady flow simulations. In the subsections below, the conservation properties of these schemes are considered. Such an analysis is useful since some unsteady flows have recently been simulated using the collocated grid system (for example, [13]).

6.1. Second Order Accurate Schemes in a Collocated Grid System

We first consider second order accurate finite difference schemes in a collocated grid system. The discrete continuity equation is centered at the definition point of p , and makes use of the interpolated flux velocity, F_i , rather than the velocity itself:

$$(Cont. - C2) \equiv \frac{\delta_1 F_i}{\delta_1 x_i} = 0. \quad (115)$$

This is similar to the procedure used in the staggered grid system. The pressure term in the momentum equation is discretized using $(Pres. - R2)_i$ of Eq. (46). This is similar to the regular grid system. Therefore, the projection stage onto a solenoidal field in the fractional step method is

$$u_i^{n+1} = u_i^* - \alpha \Delta t (Pres. - R2)_i, \quad (116)$$

$$(Cont. - C2)^{n+1} = 0. \quad (117)$$

This projection stage corresponds to Eqs. (51) and (52). In this stage, the velocity components F_i are computed via the following special interpolation formula [14]

$$F_i^{n+1} = \overline{u_i^*}^{1x_i} - \alpha \Delta t (Pres. - S2)_i. \quad (118)$$

$(Pres. - S2)_i$ is the pressure term of Eq. (78) that is used in the staggered grid system. The Poisson equation for the pressure for the collocated grid system is constructed by substituting Eq. (118) into Eq. (117) in a discrete sense.

$$\frac{\delta_1}{\delta_1 x_i} \left(\frac{\delta_1 p}{\delta_1 x_i} \right) = \frac{1}{\alpha \Delta t} \frac{\delta_1 \bar{u}_i^{*1x_i}}{\delta_1 x_i}. \quad (119)$$

The left-hand side of Eq. (119) is the same discrete form of Eq. (85) in the staggered grid system, and as a result, non-oscillatory pressure solutions are expected from this equation. The following convective schemes are equivalent if $(Cont. - C2) = 0$:

$$(Div. - C2)_i \equiv \frac{\delta_1 F_j \bar{u}_i^{1x_j}}{\delta_1 x_j}, \quad (120)$$

$$(Adv. - C2)_i \equiv \frac{\overline{\delta_1 u_i}^{1x_j}}{F_j \delta_1 x_j}, \quad (121)$$

$$(Skew. - C2)_i \equiv \frac{1}{2} (Div. - C2)_i + \frac{1}{2} (Adv. - C2)_i. \quad (122)$$

$(Adv. - C2)_i$ is connected with $(Div. - C2)_i$ through

$$(Adv. - C2)_i = (Div. - C2)_i - u_i \cdot (Cont. - C2). \quad (123)$$

$(Div. - C2)_i$ is conservative *a priori* in the momentum equation. The product between u_1 and $(Skew. - C2)_1$ can be written as

$$u_1 \cdot (Skew. - C2)_1 = \frac{\delta_1 F_j \widetilde{u_1 u_i}^{1x_j} / 2}{\delta_1 x_j}. \quad (124)$$

Therefore, $(Skew. - C2)_1$ is conservative in the transport equation of $u_1^2/2$. In the same way, $(Skew. - C2)_i$ is conservative *a priori* in the transport equation of kinetic energy K . Using Eq. (123), the conservation properties of $(Div. - C2)_i$, $(Adv. - C2)_i$, and $(Skew. - C2)_i$ are determined. The result is that $(Div. - C2)_i$, $(Adv. - C2)_i$, and $(Skew. - C2)_i$ are fully conservative provided $(Cont. - C2) = 0$.

Next, we investigate the pressure term in a collocated grid system. The pressure term is discretized using $(Pres. - R2)_i$, which was shown in Eq. (49) to be conservative in the transport equation of kinetic energy if $(Cont. - R2) = 0$. However, the collocated continuity equation is $(Cont. - C2) = 0$ and thus $(Pres. - R2)_i$ is not locally kinetic energy conserving in a collocated grid system. In addition, it can be shown that $(Pres. - R2)_i$ is not globally conservative either in a collocated grid system. It can be shown that the difference between $(Cont. - R2)$ and $(Cont. - C2)$ scales like

$$(Cont. - R2) - (Cont. - C2) = O(\Delta t \cdot h^2). \quad (125)$$

Therefore, the pressure term has a conservation error of $O(\Delta t \cdot h^2)$ in the transport equation of kinetic energy. As will be shown in the following section, the conservation error appears to be dissipative and thus the collocated grid scheme may be stable although still affected by conservation error. Table 10 shows the conservation properties for the second order accurate finite difference schemes in a collocated grid system.

TABLE 10
Conservation Properties of Second Order Accurate Finite Difference
Schemes in a Collocated Grid System

FD schemes for momentum eq.	Transport equations		
	u_i	$u_i^2/2$	K
(Div. - C2)	○	○	○
(Adv. - C2)	○	○	○
(Skew. - C2)	○	○	○
(Pres. - R2)	○	×	▽

Note. ○ is conservative *a priori*, ○ is conservative if $(Cont. - C2) = 0$, × is not conservative. ▽ has an error of $O(\Delta t \cdot h^2)$ even if $(Cont. - C2) = 0$.

6.2. Fourth Order Accurate Schemes in a Collocated Grid System

Next, we outline fourth order accurate finite difference schemes in a collocated grid system. The continuity is discretized in the same way as Eq. (79) of the staggered grid system, but using the interpolated flux velocities:

$$(Cont. - C4) \equiv \frac{9}{8} \frac{\delta_1 F_i}{\delta_1 x_i} - \frac{1}{8} \frac{\delta_3 F_i}{\delta_3 x_i} = 0. \quad (126)$$

Fourth order accurate equations corresponding to Eqs. (116), (117), and (118) are

$$u_i^{n+1} = u_i^* - \alpha \Delta t (Pres. - R4)_i, \quad (127)$$

$$(Cont. - C4)^{n+1} = 0, \quad (128)$$

$$F_i^{n+1} = \left(\frac{9}{8} \overline{u_i^*}^{1x_i} - \frac{1}{8} \overline{u_i^*}^{3x_i} \right) - \alpha \Delta t (Pres. - S4)_i. \quad (129)$$

The Poisson equation for the pressure resulting from Eqs. (128) and (129) is

$$\begin{aligned} & \frac{9}{8} \frac{\delta_1}{\delta_1 x_i} \left(\frac{9}{8} \frac{\delta_1 p}{\delta_1 x_i} - \frac{1}{8} \frac{\delta_3 p}{\delta_3 x_i} \right) - \frac{1}{8} \frac{\delta_3}{\delta_3 x_i} \left(\frac{9}{8} \frac{\delta_1 p}{\delta_1 x_i} - \frac{1}{8} \frac{\delta_3 p}{\delta_3 x_i} \right) \\ &= \frac{1}{\alpha \Delta t} \frac{9}{8} \frac{\delta_1}{\delta_1 x_i} \left(\frac{9}{8} \overline{u_i^*}^{1x_i} - \frac{1}{8} \overline{u_i^*}^{3x_i} \right) - \frac{1}{\alpha \Delta t} \frac{1}{8} \frac{\delta_3}{\delta_3 x_i} \left(\frac{9}{8} \overline{u_i^*}^{1x_i} - \frac{1}{8} \overline{u_i^*}^{3x_i} \right). \end{aligned} \quad (130)$$

The convective schemes that are equivalent if $(Cont. - C4) = 0$ are

$$(Div. - C4)_i \equiv \frac{9}{8} \frac{\delta_1 F_j \bar{u}_i^{1x_j}}{\delta_1 x_j} - \frac{1}{8} \frac{\delta_3 F_j \bar{u}_i^{3x_j}}{\delta_3 x_j}, \quad (131)$$

$$(Adv. - C4)_i \equiv \frac{9}{8} \frac{\overline{F_j \delta_1 u_i}}{\delta_1 x_j}^{1x_j} - \frac{1}{8} \frac{\overline{F_j \delta_3 u_i}}{\delta_3 x_j}^{3x_j}, \quad (132)$$

$$(Skew. - C4)_i \equiv \frac{1}{2} (Div. - C4)_i + \frac{1}{2} (Adv. - C4)_i. \quad (133)$$

TABLE 11
Conservation Properties of Fourth Order Accurate Finite Difference
Schemes in a Collocated Grid System

FD schemes for momentum eq.	Transport equations		
	u_i	$u_1^2/2$	K
(Div. - C4)	⊖	○	○
(Adv. - C4)	○	○	○
(Skew. - C4)	○	⊖	⊖
(Pres. - R4)	⊖	×	∇

Note. ⊖ is conservative *a priori*, ○ is conservative if $(Cont. - C4) = 0$, × is not conservative. ∇ has an error of $O(\Delta t \cdot h^4)$ even if $(Cont. - C4) = 0$.

$(Adv. - C4)_i$ is related to $(Div. - C4)_i$ via

$$(Adv. - C4)_i = (Div. - C4)_i - u_i \cdot (Cont. - C4). \quad (134)$$

$(Div. - C4)_i$ is conservative *a priori* in the momentum equation. The product between u_1 and $(Skew. - C4)_1$ can be rewritten as

$$u_1 \cdot (Skew. - C4)_1 = \frac{9}{8} \frac{\delta_1 F_j \widetilde{u_1 u_1}^{1x_j} / 2}{\delta_1 x_j} - \frac{1}{8} \frac{\delta_3 F_j \widetilde{u_1 u_1}^{3x_j} / 2}{\delta_3 x_j}. \quad (135)$$

Therefore, $(Skew. - C4)_i$ is conservative *a priori* in the transport equation of $u_1^2/2$. $(Skew. - C4)_i$ is also conservative *a priori* in the transport equation of K , $u_2^2/2$ and $u_3^2/2$. Thus, the conservation properties of $(Div. - C4)_i$, $(Adv. - C4)_i$, and $(Skew. - C4)_i$ are determined. Once again, the pressure term is seen to violate kinetic energy conservation, with the error resulting from the difference between $(Cont. - R4)$ and $(Cont. - C4)$. It can be shown that this difference scales like

$$(Cont. - R4) - (Cont. - C4) = O(\Delta t \cdot h^4). \quad (136)$$

Therefore, $(Pres. - R4)_i$ leads to a conservation error of $O(\Delta t \cdot h^4)$ in the transport equation of kinetic energy. Table 11 shows conservation properties of the fourth order accurate finite difference schemes in a collocated grid system.

Finally, we note that the transport equation of a passive scalar, θ , is usually centered at the pressure node in a staggered grid system. In a collocated grid system, a similar grid arrangement exists for u_i and F_i . Thus by analogy, we can use the results of this section to infer the conservation properties for the passive scalar equation in a staggered grid system. In particular, Eqs. (120), (121), and (122) (with u_i replaced by θ and F_j replaced by U_j) are conservative second order accurate convective schemes for a passive scalar in a staggered grid system. Likewise, Eqs. (131), (132), and (133) can be used to generate conservative fourth order accurate convective schemes [4].

7. NON-UNIFORM GRID ARRANGEMENT AND BOUNDARY CONDITIONS

The preceding analysis has been conducted under the assumption of a uniform grid. In this section we generalize the analysis to non-uniform grid systems and discuss the treatment of non-periodic boundary conditions. We shall restrict our attention to the fourth order accurate schemes in a staggered grid system. Generalizations of the other schemes can be accomplished in an analogous manner. For simplicity, we also restrict our attention to meshes that are non-uniform in only one direction.

7.1. Non-uniform Grid Treatment for Fourth Order Accurate Finite Difference Schemes in a Staggered Grid System

Let y be the non-uniform direction with point distribution y_j . A straightforward extension of Eqs. (26) and (27) for differentiation and interpolation on the non-uniform mesh is

$$\frac{\delta_n \phi}{\delta_n y} \Big|_{y_j} \equiv \frac{\phi(y_{j+n/2}) - \phi(y_{j-n/2})}{y_{j+n/2} - y_{j-n/2}}, \quad (137)$$

$$\bar{\phi}^{ny} \Big|_{y_j} \equiv \frac{(y_j - y_{j-n/2})\phi(y_{j+n/2}) + (y_{j+n/2} - y_j)\phi(y_{j-n/2})}{y_{j+n/2} - y_{j-n/2}}. \quad (138)$$

Unfortunately the above formulas do not satisfy Eqs. (36) to (42), and therefore a simple replacement of the uniform mesh operators with these forms will not result in conservative schemes on a non-uniform mesh. More importantly, no operators appear to exist that result in fourth order accuracy while remaining fully conservative on a non-uniform mesh. One must therefore make a choice between strict conservation and strict fourth order accuracy. If accuracy is to be sacrificed, full conservation can be achieved on a non-uniform mesh through the use of the operators

$$\frac{\delta_n \phi}{\delta_n y} \Big|_{y_j} \equiv \frac{\phi(y_{j+n/2}) - \phi(y_{j-n/2})}{n \cdot (y_{j+1/2} - y_{j-1/2})}, \quad (139)$$

$$\bar{\phi}^{ny} \Big|_{y_j} \equiv \frac{\phi(y_{j+n/2}) + \phi(y_{j-n/2})}{2}. \quad (140)$$

These operators satisfy Eqs. (36) to (42) and therefore lead to fully conservative schemes. We shall denote the use of Eqs. (139) and (140) in the second and fourth order divergence forms as $(Div. - S2 - F)$ and $(Div. - S4 - F)$, respectively, where the $-F$ stands for *fully conservative*. Unfortunately the loss of accuracy in this formulation is substantial with $(Div. - S4 - F)$ dropping to second order on a non-uniform mesh. Note that $(Div. - S2 - F)$ is actually identical to $(Div. - S2)$ and thus retains second order accuracy, even on a non-uniform mesh.

If high order accuracy is desired, it is possible to optimize the scheme so that it remains fourth order on a non-uniform mesh at the expense of a slight conservation error. As we shall see, the conservation error itself can be limited to fourth order in the mesh spacing and thus such a scheme may still be useful even for high Reynolds number calculations.

In order to illustrate the procedure, we start with the advective form, $(Adv. - S4)$, as this form will require the least amount of modification [5]. A discrete form of $V \frac{\delta U}{\delta y}$ in $(Adv. - S4)$ on a non-uniform grid is

$$\begin{aligned} \left(V \frac{\delta U}{\delta y} \right) \Big|_j = & C_j^{1+} \cdot V_{j+1/2} \frac{U_{j+1} - U_j}{y_{j+1} - y_j} + C_j^{1-} \cdot V_{j-1/2} \frac{U_j - U_{j-1}}{y_j - y_{j-1}} \\ & + C_j^{3+} \cdot V_{j+3/2} \frac{U_{j+3} - U_j}{y_{j+3} - y_j} + C_j^{3-} \cdot V_{j-3/2} \frac{U_j - U_{j-3}}{y_j - y_{j-3}}, \end{aligned} \quad (141)$$

where the four weights are

$$C_j^{1+} = \frac{(y_{j+3} - y_j)(y_j - y_{j-3})(y_j - y_{j-1})}{[(y_{j+3} - y_j)(y_j - y_{j-3}) - (y_{j+1} - y_j)(y_j - y_{j-1})](y_{j+1} - y_{j-1})}, \quad (142a)$$

$$C_j^{1-} = \frac{(y_{j+3} - y_j)(y_j - y_{j-3})(y_{j+1} - y_j)}{[(y_{j+3} - y_j)(y_j - y_{j-3}) - (y_{j+1} - y_j)(y_j - y_{j-1})](y_{j+1} - y_{j-1})}, \quad (142b)$$

$$C_j^{3+} = \frac{(y_{j+1} - y_j)(y_j - y_{j-1})(y_j - y_{j-3})}{[(y_{j+3} - y_j)(y_j - y_{j-3}) - (y_{j+1} - y_j)(y_j - y_{j-1})](y_{j+3} - y_{j-3})}, \quad (142c)$$

$$C_j^{3-} = \frac{(y_{j+1} - y_j)(y_j - y_{j-1})(y_{j+3} - y_j)}{[(y_{j+3} - y_j)(y_j - y_{j-3}) - (y_{j+1} - y_j)(y_j - y_{j-1})](y_{j+3} - y_{j-3})}. \quad (142d)$$

$V_{j+n/2}$ and $V_{j-n/2}$ in Eq. (141) are obtained via fourth order interpolation in y at the locations $y_{j+n/2} = (y_{j+n} + y_j)/2$ and $y_{j-n/2} = (y_j + y_{j-n})/2$, respectively. They are also shifted half a cell in the x direction using fourth order interpolation (35). The interpolations are such that the scheme collapses to Eq. (102) on a uniform grid, and thus will have the desired conservation properties in this limit. On a non-uniform mesh, the scheme is fourth order accurate when grid stretching is smooth (formal accuracy is $O(h^4 + h^3 \frac{dh}{dy})$), but has a fourth order error in kinetic energy conservation. We shall refer to this scheme as $(Adv. - S4 - S)_i$, where the S denotes that the scheme is fourth order even on a stretched mesh.

7.2. Boundary Conditions

As far as non-periodic boundary conditions are concerned, we restrict our attention to a solid wall. We work in the context of *ghost points* that extend beyond the boundaries so that a consistent stencil can be used on the interior as well as near the boundaries.

The boundary conditions can be designed to ensure global momentum conservation in the non-periodic and perhaps non-uniform direction if the following discrete relation holds

$$\sum_{j=1}^N (h_y)_j \frac{\delta \phi}{\delta y} \Big|_j = \phi_{N+1/2} - \phi_{1/2}, \quad (143)$$

where $\delta \phi / \delta y$ is an arbitrary finite difference operator, and $(h_y)_j = (y_{j+1/2} - y_{j-1/2})$. $j = 1/2$ and $j = N + 1/2$ denote the lower and upper walls, respectively. We shall enforce this condition for the fully conservative scheme, $(Div. - S4 - F)$.

The viscous term requires the second derivative of streamwise velocity component, U , in the wall normal direction. This quantity is discretized as follows near the wall

$$\begin{aligned} \frac{\delta^2 U}{\delta y^2} \Big|_j &= \frac{\delta_1}{\delta_1 y} \left(\frac{\delta U}{\delta y} \Big|_j^F \right) \Big|_j, \\ \frac{\delta U}{\delta y} \Big|_{j+1/2}^F &\equiv \frac{\partial [U^L(y)|_{j+1/2}]}{\partial y} \Big|_{j+1/2} - \frac{(h_y)_j (h_y)_{j+1}}{24} \frac{\partial^3 [U^L(y)|_{j+1/2}]}{\partial y^3} \Big|_{j+1/2}, \end{aligned} \quad (144)$$

where $U^L(y)$ is the Lagrangian interpolation of U defined as

$$\begin{aligned} U^L(y)|_{j+1/2} &= \frac{(y - y_j)(y - y_{j+1})(y - y_{j+2})}{(y_{j-1} - y_j)(y_{j-1} - y_{j+1})(y_{j-1} - y_{j+2})} U_{j-1} \\ &+ \frac{(y - y_{j-1})(y - y_{j+1})(y - y_{j+2})}{(y_j - y_{j-1})(y_j - y_{j+1})(y_j - y_{j+2})} U_j \\ &+ \frac{(y - y_{j-1})(y - y_j)(y - y_{j+2})}{(y_{j+1} - y_{j-1})(y_{j+1} - y_j)(y_{j+1} - y_{j+2})} U_{j+1} \\ &+ \frac{(y - y_{j-1})(y - y_j)(y - y_{j+1})}{(y_{j+2} - y_{j-1})(y_{j+2} - y_j)(y_{j+2} - y_{j+1})} U_{j+2}. \end{aligned} \quad (145)$$

Mass conservation gives boundary conditions for the wall normal velocity components, $V_{-1/2}$ and $V_{N+3/2}$ [5]:

$$V_{-1/2} = 2V_{1/2} - V_{3/2}, \quad (146a)$$

$$V_{N+3/2} = 2V_{N+1/2} - V_{N-1/2}. \quad (146b)$$

Momentum conservation for the convection term in the streamwise velocity equation gives the following boundary conditions:

$$(\bar{V}^x \bar{U}^{3y})_{-1/2} = 27(\bar{V}^x \bar{U}^{1y})_{1/2} - (\bar{V}^x \bar{U}^{3y})_{3/2} - (\bar{V}^x \bar{U}^{3y})_{1/2} - 24V_{1/2}U_{1/2}, \quad (147a)$$

$$(\bar{V}^x \bar{U}^{3y})_{N+3/2} = 27(\bar{V}^x \bar{U}^{1y})_{N+1/2} - (\bar{V}^x \bar{U}^{3y})_{N-1/2} - (\bar{V}^x \bar{U}^{3y})_{N+1/2} - 24V_{N+1/2}U_{N+1/2}, \quad (147b)$$

$$\bar{V}^x \equiv \frac{9}{8}\bar{V}^{1x} - \frac{1}{8}\bar{V}^{3x}.$$

Boundary conditions for the streamwise velocity component, U_0 , U_{-1} , U_{N+1} , and U_{N+2} are obtained from the solution of the two equations

$$U^L(y_{j+1/2})|_{j+1/2} = U_{j+1/2}, \quad j = 0, N, \quad (148)$$

$$\left. \frac{\partial^3 [U^L(y)|_{j+1/2}]}{\partial y^3} \right|_{j+1/2} = 0, \quad j = 0, N. \quad (149)$$

For a uniform grid, the solution to these equations is

$$U_0 = \frac{8}{3}U_{1/2} - 2U_1 + \frac{1}{3}U_2, \quad (150a)$$

$$U_{-1} = 8U_{1/2} - 9U_1 + 2U_2, \quad (150b)$$

$$U_{N+1} = \frac{8}{3}U_{N+1/2} - 2U_N + \frac{1}{3}U_{N-1}, \quad (150c)$$

$$U_{N+2} = 8U_{N+1/2} - 9U_N + 2U_{N-1}. \quad (150d)$$

For a non-uniform grid, the solution will be of the same form but with the coefficients being dependent on ratios of the mesh spacings in the vicinity of the wall.

We must also specify $V_{-3/2}$ and $V_{N+5/2}$ for use in the wall normal momentum equation. These values are obtained from the mass conservation constraint applied at $j=0$ and $j=N+1$

$$V_{-3/2} = 27V_{1/2} - 26V_{3/2} - 24(h_y)_0 \left(\frac{9}{8} \frac{\delta_1 U}{\delta_1 x} - \frac{1}{8} \frac{\delta_3 U}{\delta_3 x} \right)_0, \quad (151a)$$

$$V_{N+5/2} = 27V_{N+1/2} - 26V_{N-1/2} + 24(h_y)_{N+1} \left(\frac{9}{8} \frac{\delta_1 U}{\delta_1 x} - \frac{1}{8} \frac{\delta_3 U}{\delta_3 x} \right)_{N+1}. \quad (151b)$$

Here we assume that $(h_y)_0 = (h_y)_1$ and $(h_y)_{N+1} = (h_y)_N$. The wall boundary condition for the pressure term, $\partial p / \partial y$, is constructed to satisfy the following conservation constraint

$$\sum_{j=1}^{N-1} (h_y)_{j+1/2} \frac{\delta p}{\delta y} \Big|_{j+1/2} = p_N - p_1. \quad (152)$$

This condition leads to

$$p_0 = 2p_1 - p_2, \quad (153a)$$

$$p_{N+1} = 2p_N - p_{N-1}. \quad (153b)$$

Simpler boundary conditions can be used if strict conservation is not required. In this work we use the analytical solution for Stokes flow [15] as the wall boundary condition for the fourth order advective form, (*Adv.* – *S4* – *S*). The Stokes flow boundary condition is implemented by simply requiring that $U(-y) = -U(y)$ and $V(-y) = V(y)$ near the wall at $y = 0$.

8. NUMERICAL TESTS

8.1. Periodic Inviscid Flow

To confirm the results of the previous sections with numerical tests, inviscid flow simulations are performed on a two-dimensional periodic domain. The analytical conservation requirements dictate that the total momentum, $\langle u_i \rangle$, and total kinetic energy, $\langle K \rangle \equiv \frac{1}{2} \langle v_1^2 + v_2^2 \rangle$, should be conserved in time. The continuity and momentum equation are solved with several finite difference schemes in regular, staggered, and collocated grid systems. The periodic region is $2\pi \times 2\pi$ ($L = 2\pi$), and a 16×16 mesh is used. Solenoidal initial velocity fields are generated from a stream function constructed from homogeneous random numbers. The velocity fields are normalized to $\langle v_1 \rangle = \langle v_2 \rangle = 0$ and $\langle K_0 \rangle = 1.0$. A third order Runge–Kutta scheme [16] is used for the time advancement. The Poisson equation for the pressure is solved by using fast Fourier transforms (FFT).

Figure 4 shows the error of the total kinetic energy, $\langle K - K_0 \rangle$, after an integration time of $10L/(2\pi\sqrt{\langle K_0 \rangle})$, for the proper second order finite difference scheme in a staggered grid system. Kinetic energy is not conserved exactly since the third order Runge–Kutta time stepping method introduces a slight dissipative error. As expected, the time stepping error decreases with the cube of Δt , and we observe no violation of kinetic energy conservation due to the spatial scheme. The same behavior is observed in the solutions of the other proper schemes in regular and staggered grid systems.

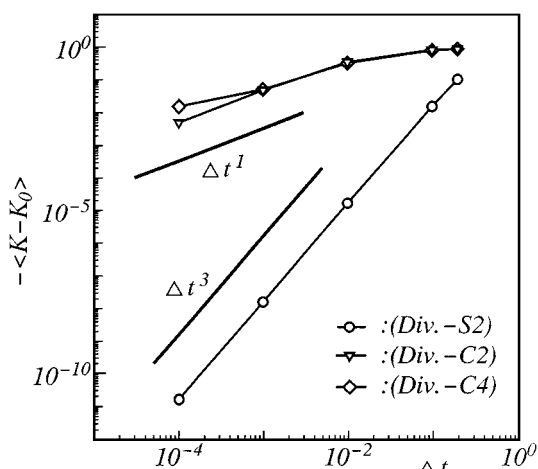


FIG. 4. Kinetic energy conservation error as a function of time step for several finite difference schemes.

TABLE 12
Kinetic Energy Conservation Error for Various Finite Difference
Schemes in Regular and Staggered Grid Systems

Convective schemes	$\langle K - K_0 \rangle$ at $T = 10$
$(Div. - R2)$	-0.782143×10^{-8}
$(Div. - R4)$	-0.193674×10^{-7}
$(Div. - S2)$	-0.163436×10^{-7}
$(Div. - S4)$	-0.319145×10^{-7}
$(Div. - R2S)$	$+\infty$ (<i>diverged</i>)
$(Adv. - R2S)$	$+\infty$ (<i>diverged</i>)
$(Rot. - R2S)$	-0.213400×10^{-6}
$(Skew. - R2)$	-0.782143×10^{-8}
$(Div. - S4A)$	$+0.244368 \times 10^{-1}$
$(Adv. - S4A)$	$+0.317386 \times 10^{-1}$
$(Skew. - S4A)$	-0.257874×10^{-7}
$(Adv. - S4K)$	$+0.725221 \times 10^{-1}$

Note. Consistency between the discrete continuity and pressure term with regard to the accuracy of the convection schemes and to the grid system are used. $\Delta t = 0.001$.

As predicted by Eqs. (125) and (136), both the second and fourth order finite difference schemes in a collocated grid system conserve kinetic energy only to order Δt . This scaling is verified in Fig. 4. Note that the error from the collocation scheme is dissipative in these tests and the calculation is therefore stable. It is also important to note that the conservation errors for the second and fourth order accurate finite difference schemes in a collocated grid system with $\Delta t = 0.001$ are larger than those of the proper schemes in regular and staggered grid systems with $\Delta t = 0.1$. Therefore, we do not recommend the use of the collocated grid system for high Reynolds number unsteady flow simulations.

The computational results for several other schemes in regular and staggered grid systems are shown in Table 12. A time increment of $\Delta t = 0.001$ is selected for the computations. The proper divergence forms in the regular and staggered grid systems conserve kinetic energy to within the time marching error. The corresponding proper advective and skew-symmetric forms are also seen to be conservative. The results from the standard divergence and advective forms in the regular grid system, $(Div. - R2S)$ and $(Adv. - R2S)$, diverge. $(Skew. - R2)$ is equivalent to $(Div. - R2)$, and is also conservative. Although the rotational form, $(Rot. - R2S)$, appears to give good results, the scheme does not conserve u_1^2, u_2^2, u_3^2 . Existing fourth order schemes in the staggered grid system, $(Div. - S4A)$, $(Adv. - S4A)$, and $(Adv. - S4K)$, produce errors that increase gradually with time. This indicates that the schemes are at least weakly unstable. The A-Domis type skew-symmetric form, $(Skew. - S4A)$, conserves kinetic energy, but momentum conservation is not ensured.

The results in Table 12 were generated with the appropriate combinations of the discretized continuity and pressure terms. The importance of the correct combination is illustrated in Table 13, where inconsistent continuity and pressure forms are used. It is apparent that kinetic energy is conserved only when the proper combination is used.

8.2. Evolution of Small Disturbances in Two-Dimensional Plane Channel Flow

In order to validate the order of accuracy of the schemes described in Section 7, we simulate the growth of low amplitude eigenmodes in laminar channel flow using a non-

TABLE 13

Kinetic Energy Conservation Error for (Div. – S4) with Several Combinations of the Discretized Continuity and Pressure Term in a Staggered Grid System

$(Div. - S4)$	$\langle K - K_0 \rangle$ at $T = 10$
with $(Pres. - S2) \& (Cont. - S2)$	$+0.212040 \times 10^{-1}$
with $(Pres. - S2) \& (Cont. - S4)$	$+0.182125 \times 10^{-2}$
with $(Pres. - S4) \& (Cont. - S4)$	-0.319145×10^{-7}

Note. $\Delta t = 0.001$.

uniform mesh in the wall-normal direction. We compare the computed eigenmode growth rate with the exact result obtained by solving the Orr–Sommerfeld eigenvalue problem. This procedure has been used by Malik *et al.* [17], among others, to measure the accuracy of different numerical methods.

The exact solution of the Orr–Sommerfeld problem can be written as

$$U(x, y, t) = (1 - y^2) + \varepsilon \cdot \text{Real} \left\{ \frac{d\phi(y)}{dy} \exp[i(\alpha x - \omega t)] \right\}, \quad (154)$$

$$V(x, y, t) = -\varepsilon \cdot \text{Real} \{ i\alpha\phi(y) \exp[i(\alpha x - \omega t)] \}, \quad (155)$$

where $\phi(y)$ is the disturbance eigenfunction, y is the wall normal direction ($-1 \leq y \leq +1$), α is the wavenumber in the streamwise direction, $\omega = \omega_r + i\omega_i$ is the temporal frequency, and ε is the perturbation amplitude. In this case we choose $\text{Re} = 8000$ and $\alpha = 1$. The only unstable mode has $\omega_r = 2.47075 \times 10^{-1}$ and $\omega_i = 2.66441 \times 10^{-3}$, and its eigenfunction, $\phi(y)$, is computed by the algorithm of Orszag [18]. With the eigenfunction determined, an initial velocity field is generated by taking $\varepsilon = 1 \times 10^{-5}$ and setting $t = 0$ in Eqs. (154) and (155).

Before advancing the simulations in time, the accuracy of the convective schemes are checked by simply differentiating the initial condition and comparing with the exact derivatives computed from the eigenfunction in its Chebyshev–Fourier representation. In order to establish order of accuracy, six different grid resolutions ($M \times N$), 8×16 , 16×32 , 32×64 , 64×128 , 128×256 , and 256×512 are used. We consider both uniform and stretched grids in order to verify that the order of accuracy is unaltered by mesh stretching. For the stretched grid, we use a hyperbolic-tangent function to distribute the wall normal velocity points, $Y_V(j) = y_{j+1/2}$ ($j = 0, 1, 2, \dots, N$)

$$Y_V(j) = \frac{\tanh [\gamma(2j/N - 1)]}{\tanh (\gamma)}. \quad (156)$$

The stretching parameter, γ , is taken to be 2.75. The grid is uniform in the streamwise direction ($\Delta x = 2\pi/M$). The error associated with $(Div. - S2 - F)$ is computed according to

$$\int_{-1}^{+1} \left\{ \frac{1}{M} \sum_{i=0}^{M-1} \left[(Div. - S2 - F)_1 - \left(\frac{\partial UU}{\partial x} + \frac{\partial UV}{\partial y} \right) \Big|_{x_i, y} \right]^2 \right\}^{1/2} dy. \quad (157)$$

The second term in the sum in Eq. (157) is computed analytically using Eqs. (154) and

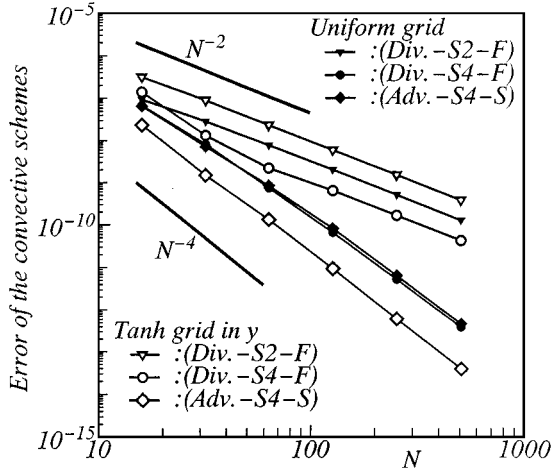


FIG. 5. Error in the numerical approximation of the convective term as a function of the number of mesh points. The test velocity field is composed of the small disturbance eigenfunction for laminar channel flow at Reynolds number 8000.

(155) at $t = 0$. The error associated with $(Div. - S4 - F)$ and $(Adv. - S4 - S)$ are computed in a similar manner.

Figure 5 shows the rate of convergence for the convective schemes $(Div. - S2 - F)$, $(Div. - S4 - F)$, and $(Adv. - S4 - S)$. The convergence rates are seen to follow the expected trends for the uniform grid. The small differences between $(Div. - S4 - F)$ and $(Adv. - S4 - S)$ for the uniform mesh case are due to differences in the wall boundary treatment. When the grid is stretched we see that $(Adv. - S4 - S)$ remains fourth order accurate, whereas $(Div. - S4 - F)$ reduces to second order. We also see that $(Div. - S2 - F)$ remains second order, even on the stretched mesh.

Next, the initial solution is advanced in time for 3.9 eigenfunction periods ($2\pi/\omega_r$) and the growth rate at the end of run is compared with the exact value. A semi-implicit time marching algorithm is used where the diffusion term in the wall normal direction is treated implicitly with the Crank–Nicolson scheme, and a third order Runge–Kutta scheme [16] is used for all other terms. The fractional step method [19] is used in order to enforce the divergence free condition. The resulting Poisson equation for the pressure is solved exactly using a Fourier Transform in the streamwise direction and either a tri- or septa-diagonal matrix algorithm in the wall normal direction for the second and fourth order schemes, respectively. The same set of 5 meshes discussed previously is used in order to determine convergence rates. The time increments for the five meshes are 0.04, 0.02, 0.01, 0.005, and 0.0025. The maximum CFL numbers are about 0.05 for all runs.

Figure 6 shows the error in the growth rate given by $(Div. - S2 - F)$, $(Div. - S4 - F)$, and $(Adv. - S4 - S)$. Again we see that $(Adv. - S4 - S)$ produces true fourth order convergence whereas $(Div. - S4 - F)$ is limited to second order.

8.3. Large Eddy Simulation of Plane Channel Flow

Further numerical tests of the schemes described in Section 7 are performed using plane channel flow. We consider fully developed incompressible flow and make use of periodic

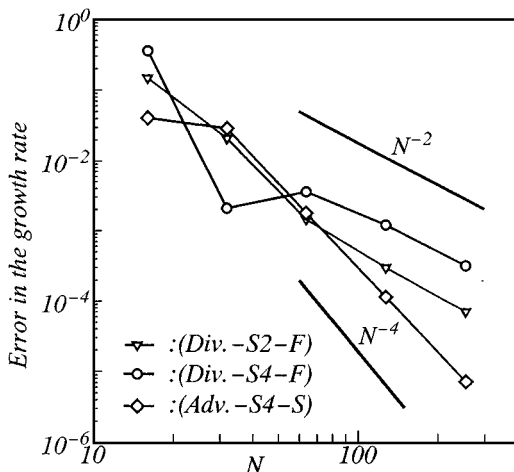


FIG. 6. Error in the eigenfunction growth rate at $t = 100$ as a function of number of mesh points.

boundary conditions in the streamwise and spanwise directions. The time marching algorithm is the same as described in the previous subsection. The dynamic subgrid scale (SGS) model [20] with the least square technique [21] and averaging in homogeneous directions is used. For the purpose of the dynamic model, test filtering is performed in the spanwise and streamwise directions. Simulations are conducted at two Reynolds numbers: $Re = 180$ and 650 , based on the channel half width and friction velocity.

Figures 7 and 8 show the profiles of mean streamwise velocity and velocity fluctuations respectively for the schemes $(Div.-S2-F)$, $(Div.-S4-F)$, and $(Adv.-S4-S)$ at $Re = 180$. Filtered DNS data [22] at the same Reynolds number are plotted as a reference in the figures. The logarithmic law for the mean velocity profile ($U^+ = 2.5 \cdot \log(y^+) + 5.5$) is also plotted in Fig. 7. In the figures, $y^+ = u_\tau y / v$ is the wall unit and $U^+ = U / u_\tau$ is mean streamwise velocity in the wall variables, u' , v' , and w' are the resolved velocity fluctuations in the streamwise, wall normal, and spanwise directions, respectively, and $\langle u'v' \rangle$ is the resolved Reynolds stress. The computational box is $4\pi \times 2 \times 4\pi/3$ and $32 \times 32 \times 32$ mesh points are used. The wall normal grid is stretched according to Eq. (156) with $\gamma = 2.40$. In this case, the grid spacings in wall units are $\Delta x^+ = 70.69$ and $\Delta z^+ = 23.56$.

The mean velocity is seen to be overpredicted in the logarithmic region when the second order scheme is used. This discrepancy is reduced when the higher order schemes are used,

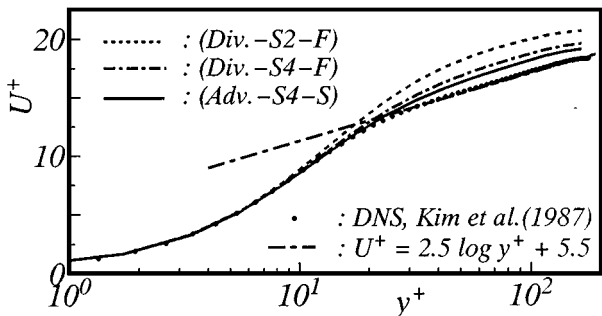


FIG. 7. Mean streamwise velocity at $Re = 180$ (LES, box $4\pi \times 2 \times 4\pi/3$, $32 \times 32 \times 32$ grid).

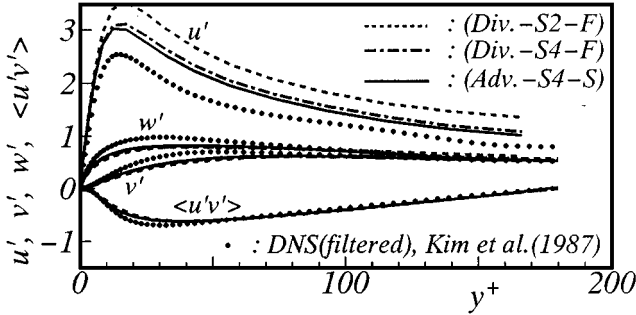


FIG. 8. Velocity fluctuations at $Re = 180$ (LES, box $4\pi \times 2 \times 4\pi/3$, $32 \times 32 \times 32$ grid).

with the true fourth order scheme, $(Adv. - S4 - S)$, giving the best results. The streamwise velocity fluctuation is overpredicted by the second order scheme whereas the spanwise and wall-normal fluctuations are underpredicted. Again these discrepancies are reduced when the higher order schemes are used with $(Adv. - S4 - S)$ giving slightly superior results.

In order to measure the effect of the numerical error unambiguously, the $Re = 180$ simulations are repeated without the use of a subgrid-scale model. In this case the results are compared with a spectral simulation (Fourier–Chebyshev–Fourier) performed with the same number of mesh points, again without a subgrid-scale model. The spectral method can be regarded as the limiting case for a higher order accurate scheme. The spectral algorithm is the Kleiser–Schumann method [23] with Werne’s modification [24], and is based on the velocity and pressure formulation. Figures 9 and 10 show the profiles of mean streamwise velocity and velocity fluctuations respectively for $(Div. - S2 - F)$, $(Div. - S4 - F)$, and $(Adv. - S4 - S)$.

The trends shown in Figs. 9 and 10 are nearly identical to those shown in Figs. 7 and 8, and thus we can conclude that the discrepancies caused by the second order method are due to the numerical error and not a shortcoming of the subgrid-scale model. We also see that the finite difference results are closer to the spectral reference case when the higher order schemes are used.

Figures 11 and 12 show the mean velocity and velocity fluctuation profiles, respectively, for $(Div. - S2 - F)$, $(Div. - S4 - F)$, and $(Adv. - S4 - S)$ at $Re = 650$. Experimental data [25] at the same Reynolds number are plotted as a reference in the figures. The logarithmic velocity profile ($U^+ = 2.5 \cdot \log(y^+) + 5.0$) is also plotted in Fig. 11. The computational

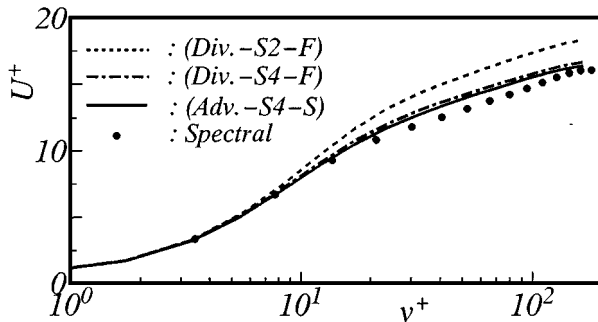


FIG. 9. Mean streamwise velocity at $Re = 180$ (No SGS model, box $4\pi \times 2 \times 4\pi/3$, $32 \times 32 \times 32$ grid).

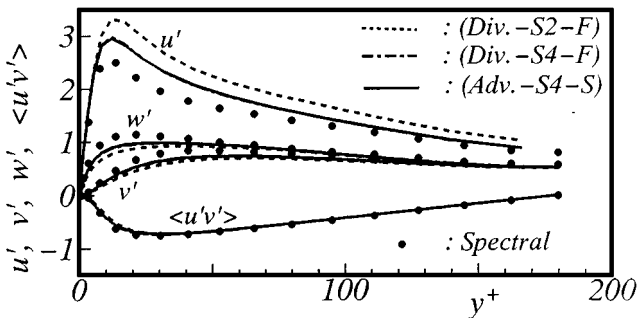


FIG. 10. Velocity fluctuations at $Re = 180$ (No SGS model, box $4\pi \times 2 \times 4\pi/3$, $32 \times 32 \times 32$ grid).

box for this case is $2\pi \times 2 \times 2\pi/3$ and $48 \times 32 \times 48$ mesh points are used. The wall-normal mesh is stretched according to Eq. (156) with $\gamma = 2.75$. The grid spacings in wall units are $\Delta x^+ = 85.08$ and $\Delta z^+ = 28.36$. The results are similar to the two previous cases with the higher order methods showing an improvement over the second order method.

9. CONCLUSIONS

Conservation of mass, momentum, and kinetic energy for incompressible flow was specified as analytical requirements for a proper set of discrete equations. Several pre-existing schemes in regular, staggered, and collocated grid systems were analyzed with regard to their conservation properties. Most of these schemes were found to violate one or more of the conservation properties. Both second and fourth order accurate fully conservative schemes were then derived where lacking for the regular and staggered mesh systems. A general procedure for constructing fully conservative schemes of arbitrary order in a staggered mesh system was also derived. Treatment for non-uniform meshes and non-periodic boundary conditions was given in detail for the new fourth order staggered mesh scheme. It was found that strict conservation and strict fourth order accuracy could not be obtained simultaneously on a non-uniform mesh. Accordingly, two alternative schemes were derived. The first is fully conservative but only formally second order accurate on a stretched mesh. The second is formally fourth order accurate on a stretched mesh but has a fourth order violation in kinetic energy conservation. The two schemes become identical on a uniform mesh where they are simultaneously conservative and fourth order accurate. Numerical tests on a non-uniform

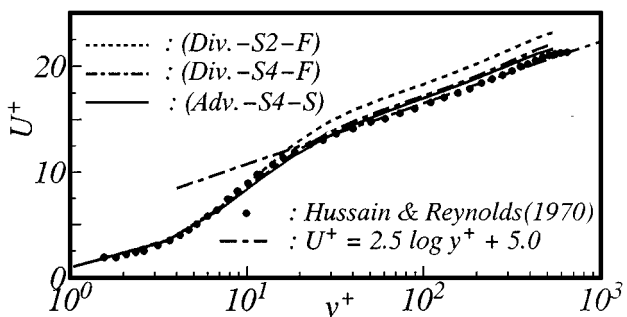


FIG. 11. Mean streamwise velocity at $Re = 650$ (LES, box $2\pi \times 2 \times 2\pi/3$, $48 \times 32 \times 48$ grid).

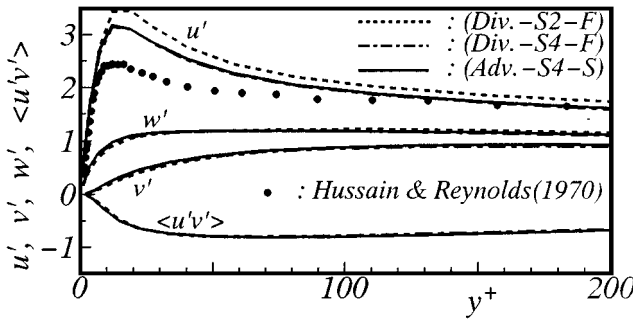


FIG. 12. Velocity fluctuations at $Re = 650$ (LES, box $2\pi \times 2 \times 2\pi/3$, $48 \times 32 \times 48$ grid).

mesh indicated a slight superiority of the fourth order, slightly non-conservative scheme. The higher order schemes were compared with a second order scheme for turbulent channel flow simulations and both variants were found to result in a significant improvement in the computed statistics.

ACKNOWLEDGMENTS

The authors thank Dr. H. Kaltenbach for his helpful suggestions. We also thank Dr. K. Jansen, Dr. W. Cabot, and Ms. D. Spinks. Y. Morinishi was supported by the Japanese Government Research Fellowship funds while at the Center for Turbulence Research.

REFERENCES

1. A. Arakawa, Computational design for long-term numerical integration of the equation of fluid motion: Two-dimensional incompressible flow, Part I, *J. Comput. Phys.* **1**, 119 (1966).
2. F. H. Harlow and J. E. Welch, Numerical calculation of time-dependent viscous incompressible flow of fluid with free surface, *Phys. Fluids* **8**, 2182 (1965).
3. S. Ghosal, An analysis of numerical errors in large-eddy simulations of turbulence, *J. Comput. Phys.* **125**, 187 (1996).
4. M. A-Domis, Large-eddy simulation of a passive scalar in isotropic turbulence, *J. Fluid Mech.* **104**, 55 (1981).
5. T. Kajishima, Conservation properties of finite difference method, *Trans. JSME* **60-574B**, 2058 (1994). [In Japanese]
6. P. Beaudan and P. Moin, *Flow Past a Circular Cylinder at Sub-Critical Reynolds Number*, Rep. TF-62, Thermosciences Div., Dept. Mech. Eng., Stanford University, Stanford, CA, 1995.
7. C. Canuto, M. Y. Hussaini, A. Quarteroni, and S. A. Zang, *Spectral Methods in Fluid Dynamics* (Springer-Verlag, New York/Berlin, 1988).
8. J. Kim and P. Moin, Application of a fractional-step method to incompressible Navier-Stokes equations, *J. Comput. Phys.* **59**, 308 (1985).
9. P. Moin and J. Kim, Numerical investigation of turbulent channel flow, *J. Fluid Mech.* **118**, 341 (1982).
10. K. Horiuti, Comparison of conservative and rotational forms in large eddy simulation of turbulent channel flow, *J. Comput. Phys.* **71**, 343 (1987).
11. K. Horiuti, Anisotropic representation of the Reynolds stress in large eddy simulation of turbulent channel flow, in *Proc. of Int. Symp. Comp. Fluid Dynamics, Nagoya*, (1989), p. 233.
12. S. A. Piacsek and G. P. Williams, Conservative properties of convection difference schemes, *J. Comput. Phys.* **6**, 392 (1970).
13. Y. Zang, R. L. Street, and J. R. Koseff, A non-staggered grid, fractional step method for time-dependent incompressible Navier-Stokes equations in curvilinear coordinates, *J. Comput. Phys.* **114**, 18 (1994).

14. C. M. Rhie and W. L. Chow, A numerical study of the turbulent flow past an isolated airfoil with trailing edge separation, *AIAA J.* **21**, 1525 (1983).
15. H. K. Moffat, Viscous and resistive eddies near a sharp corner, *J. Fluid Mech.* **18**, 1 (1964).
16. A. Wray, *Private communication*, NASA-Ames Research Center, Moffett Field, CA, 1986.
17. T. R. Malik, T. A. Zang, and M. Y. Hussaini, A spectral collocation method for the Navier-Stokes equations, *J. Comput. Phys.* **61**, 64 (1985).
18. S. A. Orszag, Accurate solution of the Orr-Sommerfeld stability equation, *J. Fluid Mech.* **50**(4), 689 (1971).
19. J. K. Dukowicz and A. S. Dvinsky, Approximation as a high order splitting for the implicit incompressible flow equations, *J. Comput. Phys.* **102**, 336 (1992).
20. M. Germano, U. Piomelli, P. Moin, and W. H. Cabot, A dynamic subgrid-scale eddy viscosity model, *Phys. Fluids A* **3**, 1760 (1991).
21. D. Lilly, A proposed modification of the Germano subgrid scale closure method, *Phys. Fluids A* **4**, 633 (1992).
22. J. Kim, P. Moin, and R. Moser, Turbulence statistics in fully developed channel flow at low Reynolds number, *J. Fluid Mech.* **177**, 133 (1987).
23. L. Kleiser and U. Schumann, Treatment of incompressibility and boundary conditions in 3-D numerical spectral simulations of plane channel flows, in *Proceedings, 3rd-GAMM Conf. on Numerical Methods in Fluid Mechanics* (1980), p. 165.
24. J. Werne, Incompressibility and no-slip boundaries in the Chebyshev-tau approximation: Correction to Kleiser and Schumann's influence-matrix solution, *J. Comput. Phys.* **120**, 260 (1995).
25. A. K. M. F. Hussain and W. C. Reynolds, *The Mechanics of a Perturbation Wave in Turbulent Shear Flow*, AFSOR Report, 70-1655TR, 1970.